

# InSAR time-series monitoring of ground displacement trends in an industrial area (Oreokastro—Thessaloniki, Greece): detection of natural surface rebound and new tectonic insights

Nikos Svigkas<sup>1,2</sup>  · Ioannis Papoutsis<sup>2</sup> · Constantinos Loupasakis<sup>3</sup> · Paraskevas Tsangaratos<sup>3</sup> · Anastasia Kiratzi<sup>1</sup> · Charalampos Haris Kontoes<sup>2</sup>

Received: 8 July 2016 / Accepted: 20 February 2017  
© Springer-Verlag Berlin Heidelberg 2017

**Abstract** The industrial area of Oreokastro, NW of the city of Thessaloniki, is monitored using radar interferometry to determine the spatial evolution of the underlying ground deformation trends. Previous studies, using SAR data acquired between 1992 and 1999, have revealed subsidence; however, the driving mechanism has not been, so far, solidly explained. Here, SAR satellite data from ERS 1, 2 and ENVISAT missions, acquired between 1992 and 2010, are analysed to enhance our understanding of the ground displacement trends and provide a thorough interpretation of the phenomena. The analysis confirms a subsiding displacement pattern from 1992 to 1999, whereas the recent data indicate that after 2003 the motion direction has changed to uplift. This whole monitoring of subsidence and the subsequent uplift is a rarely documented phenomenon, and in the case of Oreokastro is not reflecting a natural process; on the contrary, the driver is anthropogenic, related to the regional aquifer activity. Our study also highlights the fact that the local faults act as

groundwater barriers and captures the existence of a possible previously unknown tectonic structure.

**Keywords** Hazard monitoring · SAR time-series · Natural surface rebound

## Introduction

Thessaloniki (Fig. 1) is the second largest city in Greece, after the capital Athens. It is located in the northern part of the Hellenic territory at an area with alternating topography, and it is washed by the sea at Thermaikos Gulf (a semi-enclosed area of the eastern Mediterranean). It is a major economic hub and the most important city of the Balkans in terms of trade activities since the years of the Roman Empire. Thessaloniki has a rich multicultural history that has left its footprints until today, it is a major educational centre in Greece, it constitutes a junction of the Balkans and is also a metropolitan area with more than 1,000,000 inhabitants. In view of the above, the city provides a solid motivation for Natural Hazard monitoring. A significant number of important industries were established around Thessaloniki over the years. Nowadays, many of these industries no longer exist, reflecting in part the aftermath of the fiscal crisis.

The focus of the present study is the industrial area southern of Oreokastro (Fig. 1), which is a suburb north of Thessaloniki. Previous studies, covering the period 1992–1999, indicated that the broader region of Oreokastro (e.g. Galini) (Fig. 1) was subsidizing, but sufficient interpretation of the mechanism was not provided. Synthetic aperture radar (SAR) satellites had been used in the past for various applications (e.g. Battazza et al. 2009; Sonobe et al. 2014). In this study, the interferometric synthetic aperture

---

**Electronic supplementary material** The online version of this article (doi:10.1007/s12665-017-6517-9) contains supplementary material, which is available to authorized users.

---

✉ Nikos Svigkas  
svigkas@geo.auth.gr

- <sup>1</sup> Department of Geophysics, Aristotle University of Thessaloniki, 54124 Thessaloniki, Greece
- <sup>2</sup> Institute of Space Applications and Remote Sensing, National Observatory of Athens, Metaxa & Vas. Pavlou, 15236 Athens, Greece
- <sup>3</sup> Laboratory of Engineering Geology and Hydrogeology, Department of Geological Sciences, School of Mining and Metallurgical Engineering, National Technical University of Athens, Zographou Campus, Heron Polytechniou 9, 157 80 Athens, Greece

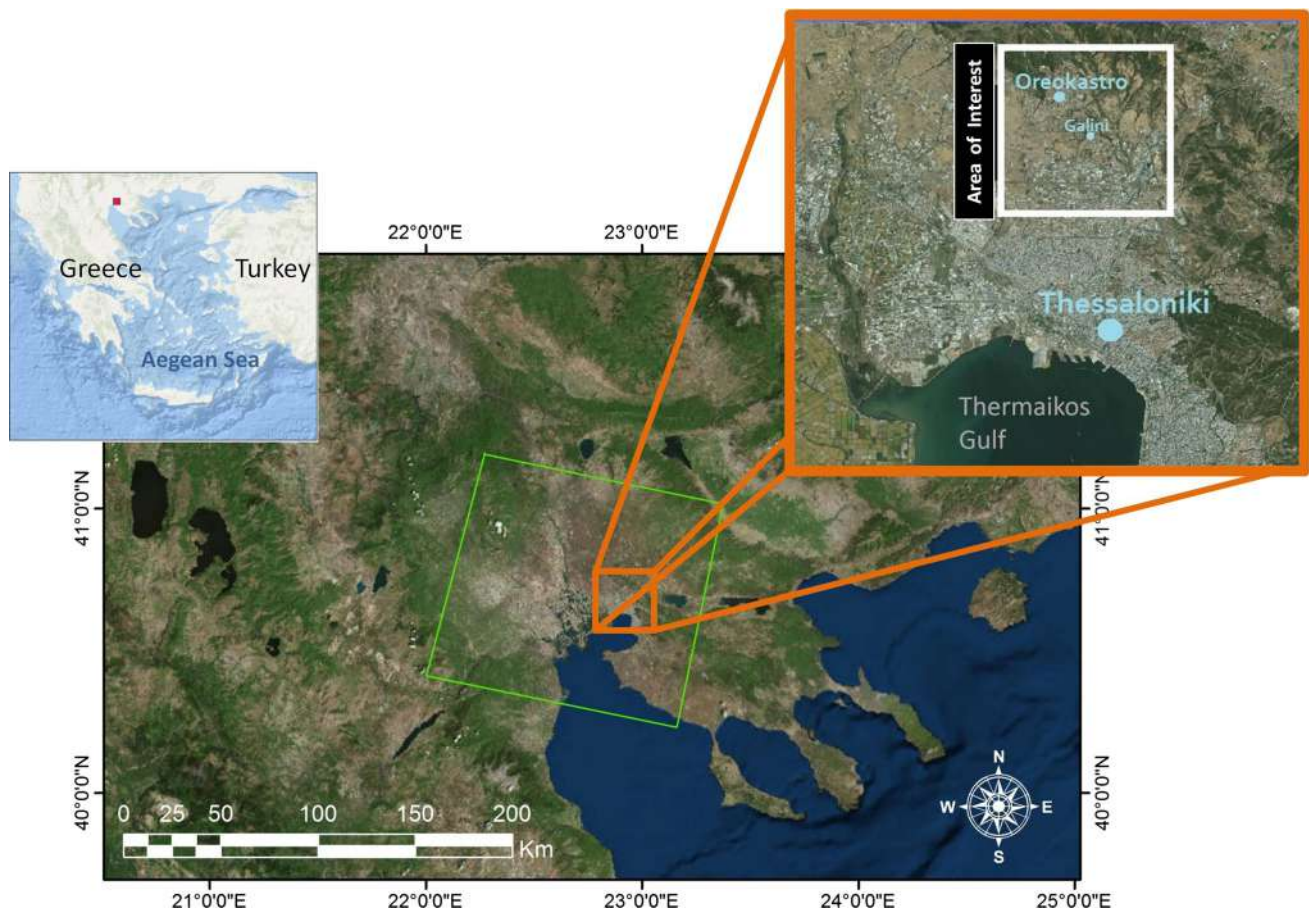


**Fig. 1** Broader region, and the focus region of study, where Oreokastro and Galini are shown in the *inset*, north of the metropolitan area of Thessaloniki. The *green rectangle* shows the

ERS and ENVISAT satellite frame. In the *inset map* of Greece to the *upper left*, the broader study area is denoted with the *red rectangle*

radar (InSAR) technology is used to study in detail the deformation pattern, deformation history and also interpret the deformation mechanism of the study area. InSAR monitoring is a remote sensing technique that exploits radar images to estimate the surface deformation. Here, the complete deformation history from 1992 to 2010, exploiting ERS 1, 2 and ENVISAT satellite missions, is presented. Interpretation of the deformation mechanisms and on the ambiguous deforming signals of the industrial area of Oreokastro is attempted. Moreover, the tectonic and the hydrogeological setting of the site correlated with the deformation phenomena is discussed. Also, via the InSAR monitoring, a previously unknown tectonic structure is revealed.

### Geology and seismicity of the study area

The broader area of Oreokastro lies mainly on Neogene formations. The urban fabric of the town is located on Pliocene lake and fluvial deposits, consisting of red clays

**Fig. 2** Geology of Oreokastro and the surrounding area. The focus region of our study is within the *blue rectangle*. The location of the two geotechnical drills below is noted on the map with *white triangles*. Borehole data are archives of the Directory of Environment, Thessaloniki Prefecture. Map is from EPPO (1996), Neotectonic Map of Greece, Thessaloniki sheet

intercalated by sands, pebble gravels and marls, and at a lesser extent of Pre-Alpine carbonate rocks and schists (Fig. 2). Two available drill profiles within the industrial zone of Oreokastro show Pliocene clays intercalated by sand, lying above the Pre-Alpine bedrock. The previously described stratigraphy contains a system of successive confined aquifers, which prior to the installation of the industries, were artesian.

The faults of the area are part of the broader tectonic regime of the Mygdonian graben. The governing extensional stresses are expressed with normal faulting and seismicity all over the area most of which is localized within the graben (Fig. 3).

Two main tectonic structures cross south of Oreokastro (Figs. 2, 3), the extension of Asvestochori fault (fault

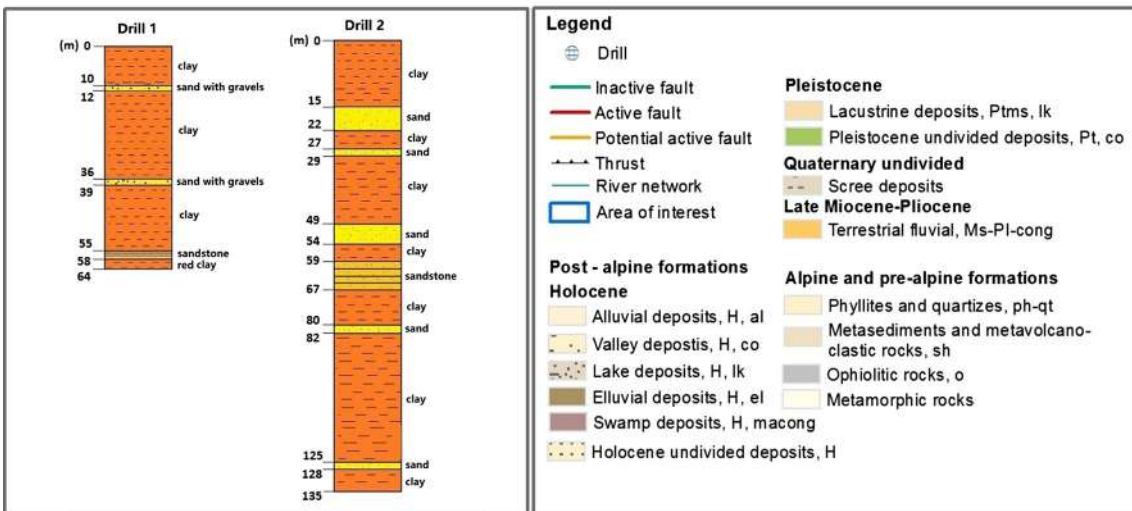
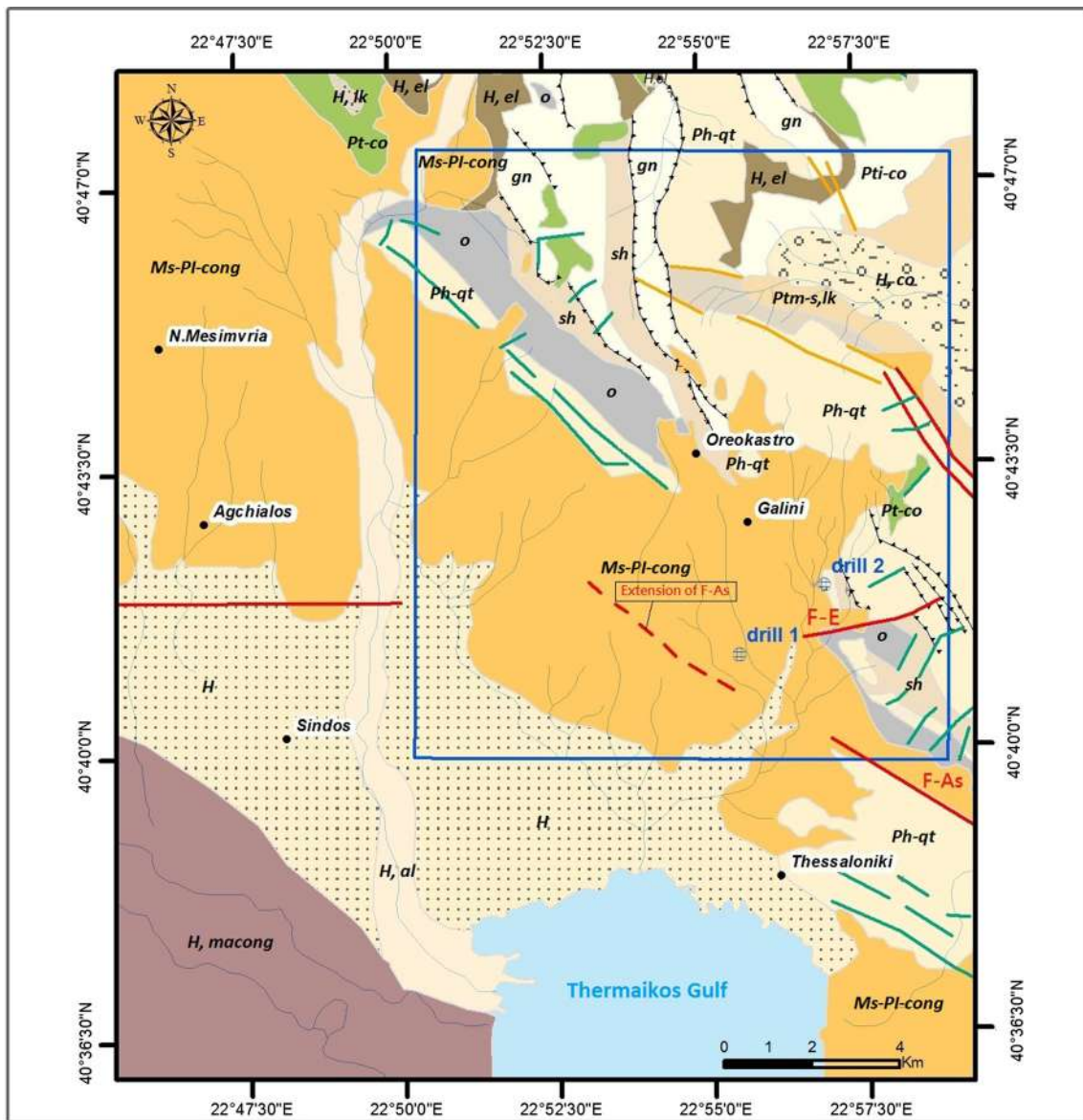
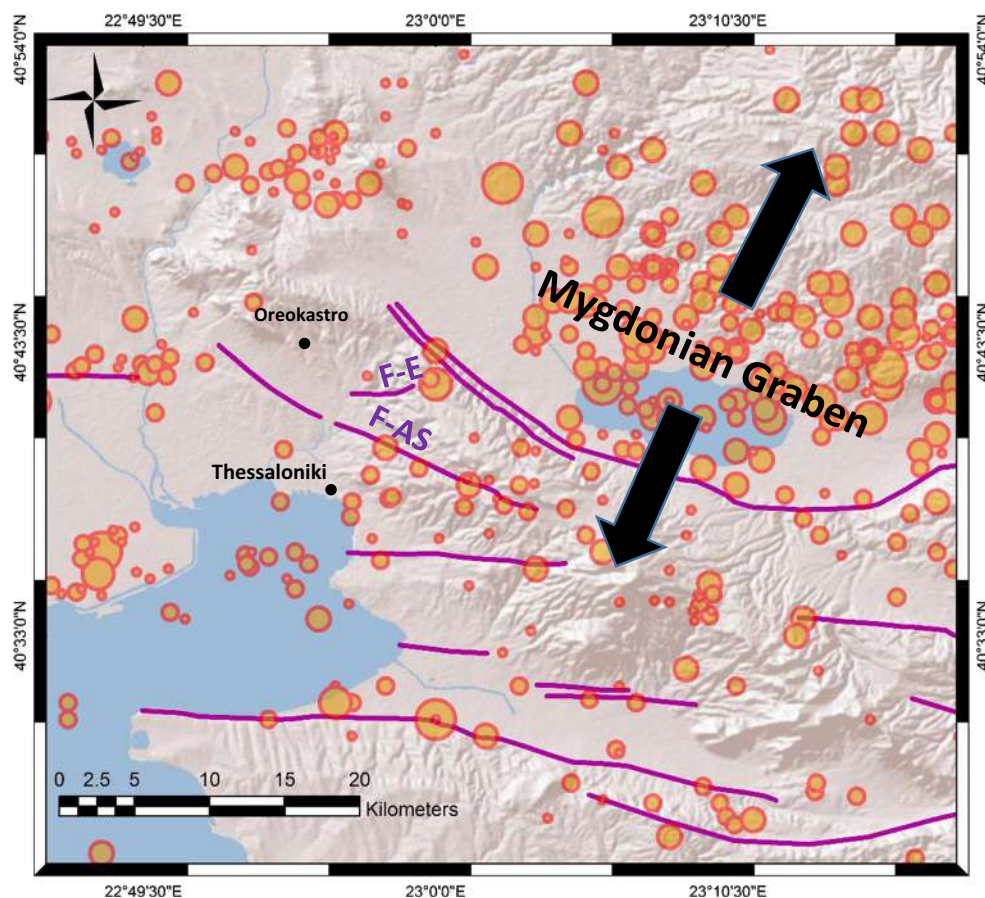


**Fig. 3** Location of Thessaloniki and Oreokastro, alongside the two main tectonic features of F–As and F–E, in terms of the broader regional tectonic pattern. Most of the seismicity is located in Mygdonian Graben which is under an extensional stress regime



F–As) and the Efkarpiya fault (fault F–E) (Zervopoulou 2010; Zervopoulou and Pavlides 2005). The Asvestochori fault, at the northern side of the city of Thessaloniki, follows the Exochi–Asvestochori axis and crosses south of the study area. This is a normal fault that is considered by structural geologists as potentially active (Zervopoulou 2010). The Efkarpiya fault is located at the northern part of the city close to the Efkarpiya suburb, at a distance of  $\sim 6$  km from the city centre. This structure is also considered as potentially active (Zervopoulou 2010). No strong earthquakes have been recorded during the instrumental period; however, the abundant microseismicity (e.g. Papazachos et al. 2000; Paradisopoulou et al. 2006; Garlaouni et al. 2015) renders these structures, from a seismological point of view, to be considered as active.

### Previous studies in the Oreokastro area

The deforming pattern detected in the region south of Oreokastro attracted the attention of many researchers (Raucoules et al. 2008; Mouratidis 2010; Zervopoulou

2010; Mouratidis et al. 2011; Sviggas et al. 2015; Costantini et al. 2016). Raucoules et al. (2008) were the first to find a deforming signal during the period 1992–1999 ( $-10$  to  $-20$  mm/year) using radar interferometry. Prior to the InSAR studies, the area was not known to deform. Previous hypotheses regarding the nature of the deformation were mainly related to the tectonic activity and the microseismicity (Raucoules et al. 2008; Mouratidis 2010; Mouratidis et al. 2011). Zervopoulou (2010) mentions that in 2006 there were cracks reported on the buildings of the area that can be attributed either to aseismic slip or to overpumping. The aforementioned studies had a significant contribution to the investigation of the phenomenon, although only the work of Zervopoulou (2010) had a considerable focus on Oreokastro. In most cases, the reference to this area was a subpart of a more general study, usually about northern Greece. That is why, even though these studies were complete, when it comes to the interpretation of the driving mechanism of the detected deformation pattern, there is a lack of proof and of a clear and systematic answer. Raucoules et al. (2008) were the first to detect

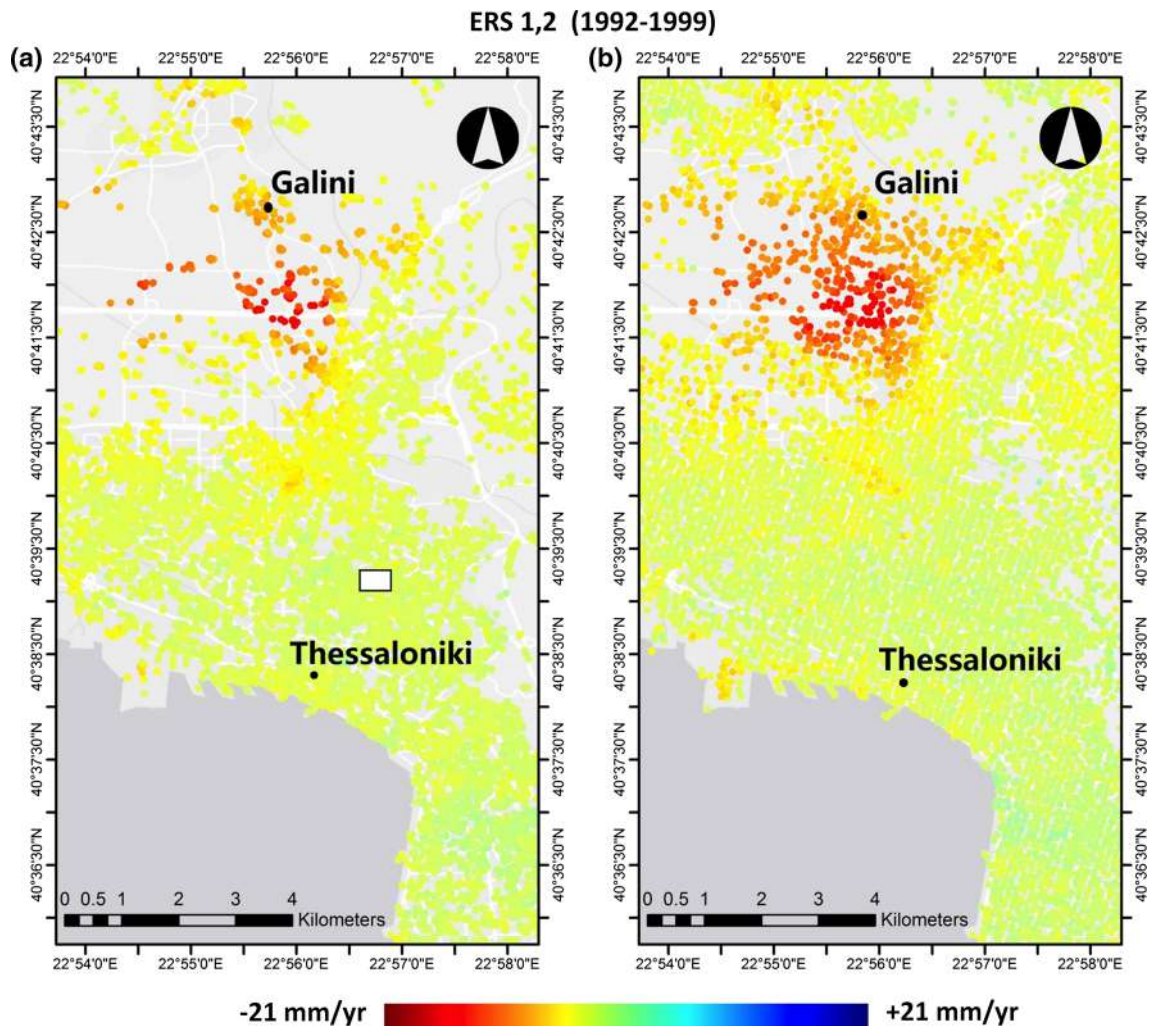


**Fig. 4** Results of the **a** PS and **b** SBAS analysis for the period 1992–1999. The metropolitan area of Thessaloniki is stable. The largest deformation signal is detected southern of Oreokastro close to

Galini (up to  $-21$  mm/year). The white rectangle in **(a)** shows the reference area used for the SAR processing. As it can be seen, the results of the PS and SBAS techniques are highly correlated

subsidence in the region; and in their preliminary study Svigkas et al. (2015) were the first to detect an uplifting pattern for the period of 2003–2010. This change in the deformation pattern is the motivation of the present work, which seeks a more in depth and detailed analysis of the deformation pattern observed at the industrial area of Oreokastro, spanning two decades, alongside a plausible interpretation of the driving mechanism.

**Methods and approach**

InSAR techniques have been broadly used for the detection of the deformation that occurs on the earth’s surface (e.g. Zebker and Goldstein 1986; Gabriel et al. 1989;

Wright and Stow 1999; Burgmann et al. 2000; Wright et al. 2001; Colesanti et al. 2003) for applications on landslides (e.g. Colesanti and Wasowski 2006; Farina et al. 2006; Bianchini et al. 2012; Bovenga et al. 2012; Cigna et al. 2012a, b; Herrera et al. 2013; Liu et al. 2013), earthquakes (e.g. Wright et al. 1999, 2003; Parsons et al. 2006), volcanoes (Amelung et al. 2000; Lanari et al. 2004; Brunori et al. 2013). This scientific tool has also contributed effectively to the monitoring of aquifer activity (e.g. Ikehara and Phillips 1994; Amelung et al. 1999; Galloway et al. 1999; Bell et al. 2008; Taniguchi et al. 2009; Lu and Danskin 2001; Chen et al. 2007; Raspini et al. 2013, 2014; Ishitsuka et al. 2014; Svigkas et al. 2016) and is considered as an important input for hydrogeological research. More on the fundamentals about SAR

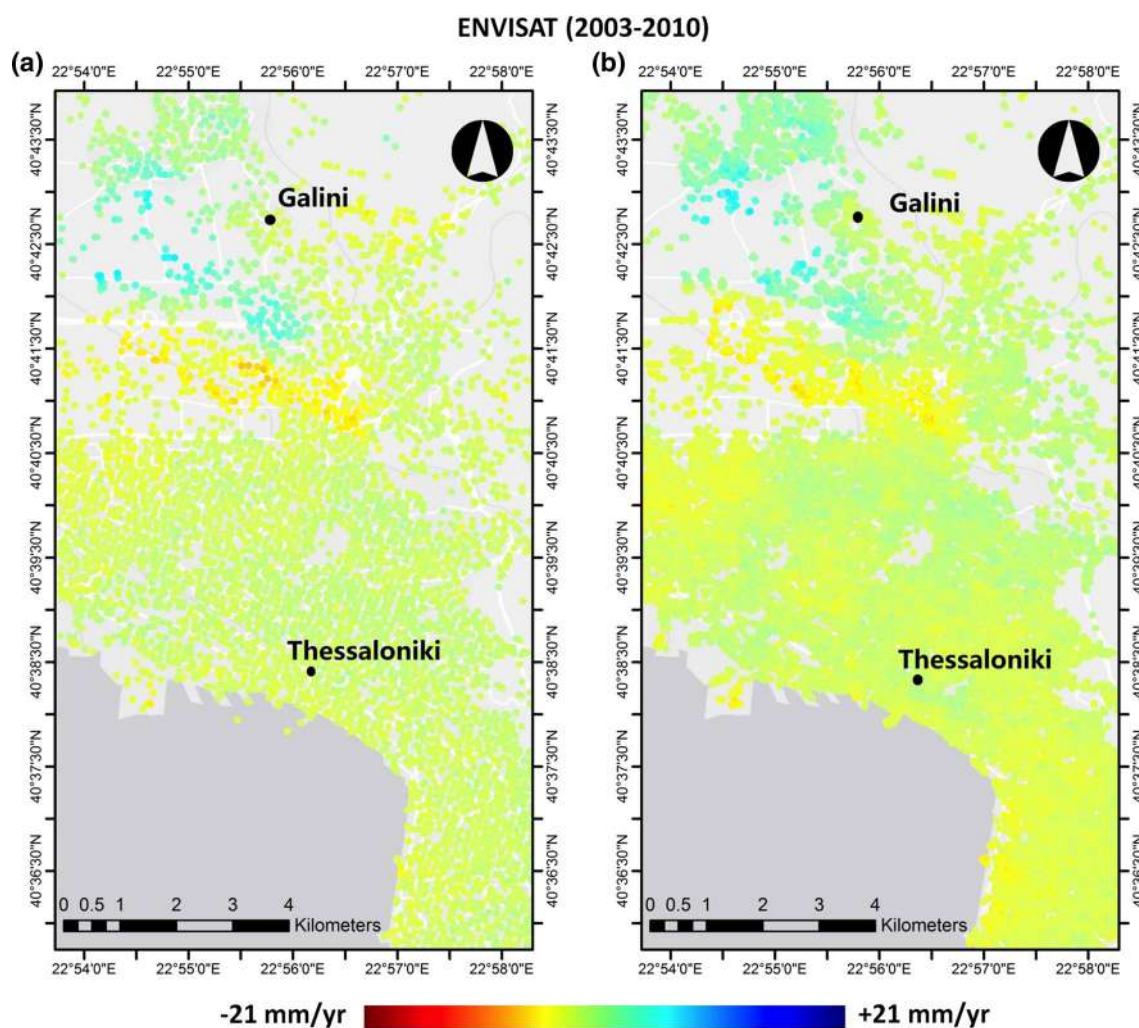


**Fig. 5** Results of the SAR time-series analysis for the period 2003–2010. **a** PS results, **b** SBAS results. Again there is high correlation between the results of the two techniques. The interesting fact is that in the study area close to Galini during the second decade

there is an uplifting trend that is opposed to the deformation pattern of the 1990s. The maximum detected uplifting value is about +9 mm/year

Interferometry can be found in Massonnet et al. (1993), Dixon (1994), Massonnet (1997), Massonnet and Feigl (1998).

In time-series techniques, radar images that spread in time are processed in pairs and these form the differential interferograms. Each point of a differential interferogram represents a phase difference between the two satellite acquisitions. This phase difference is contaminated with noisy signals, present due to temporal and geometric decorrelation effects and because of atmosphere perturbations between successive image acquisitions. Following a number of corrections (orbits, digital elevation model, changes in atmosphere) and filtering, the phase difference of each point is translated to surface displacements. Here,

we use time-series of SAR Images. Over the years, many techniques were developed (Kampes and Usai 1999; Bernardino et al. 2002; Arnaud et al. 2003; Mora et al. 2003; Lanari et al. 2004; Hooper et al. 2004, 2007; Duro et al. 2005; van der Kooij et al. 2006; Costantini et al. 2008; Ketelaar 2009). The implemented techniques herein are the small baseline subset (SBAS) (Bernardino et al. 2002), the permanent scatterers (PS) interferometry (Ferretti et al. 2000, 2001) and a hybrid approach merging both estimation worlds (Hooper 2006; Hooper et al. 2007). PS and SBAS methods exploit stacks of the differential interferograms that are formed based on connections of the satellite acquisitions. The PS approach is ideal for the urban fabric due to its high accuracy on selected stable targets, while

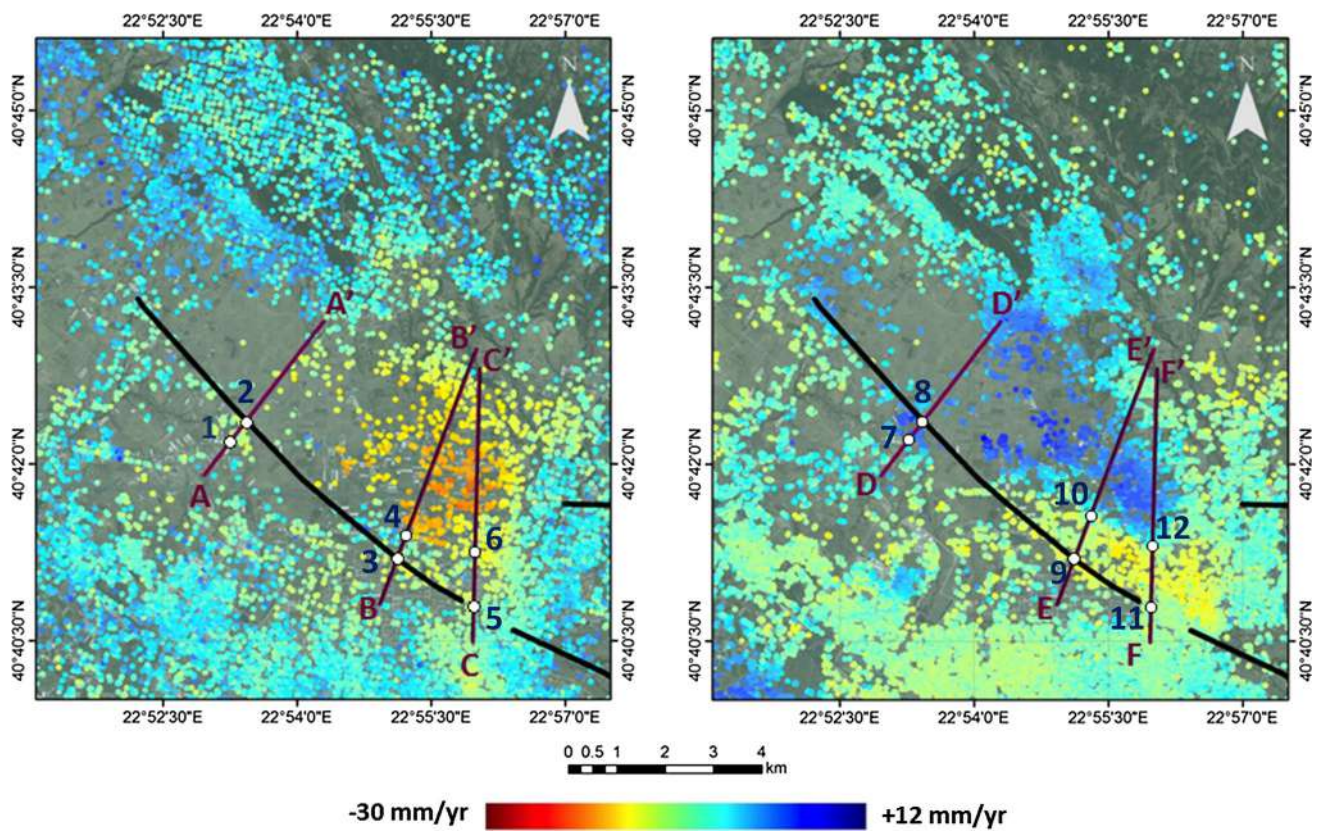


**Fig. 6** Combined results of the PS and SBAS techniques of the broader area of Oreokastro. Known faults (*black continuous lines*) from Ganas et al. (2013). During 1992–1999 (*left*) the maximum subsidence value is 21 mm/year, and during the second decade (*right*) the maximum uplifting value is 9 mm/year. The faults appear to

interact with the deformation pattern; they act as groundwater barriers. Traces A–A', B–B', C–C', D–D', E–E', F–F' on the two maps are the velocity cross sections and the topography profile presented in Fig. 12a–f. Points 1–12 are selected locations (see “New tectonic insights” section in the paper)

SBAS is more appropriate for tectonic studies, allowing the collection of millimetric measurements over a broader deforming surface (Sousa et al. 2011). A combination of the two approaches gives a better definition of the deforming pattern of an area. The theoretical precision of the methods presented in this study for ground velocity estimation is of the order of 1 mm/year. However, considering the nonlinear phenomena identified in the region, the precision of the velocity estimates can rise up to 2 mm/year.

**Data and software**

ERS 1,2 (46 level\_0 Images) and ENVISAT (37 level\_0 images) data both from track 279 covering the period 1992–1999 and 2003–2010, respectively, courtesy of the European Space Agency (ESA) were exploited. For the analysis, orbital data were used from Delft University of Technology and VOR data were offered by ESA. The datasets and the connection graphs of the radar images used

in the SAR analysis procedure are presented in the Online Resources of the study. Topographic corrections were based on the SRTM Digital Elevation Model V3, 90-m spatial resolution (e.g. Farr and Kobrick 2000), and the mass processing was conducted with the StaMPS (Stanford Method for Persistent Scatterers) algorithm (Hooper 2006; Hooper et al. 2007) and also with the software SARscape (from Sarmap, CH). Prior to the time-series processing with StaMPS, the focusing was accomplished with ROI\_PAC (Repeat Orbit Interferometry Package), developed by California Institute of Technology and Jet Propulsion Laboratory (NASA), and the interferograms were generated with DORIS (Delft Object-Oriented Radar Interferometric Software).

**Results**

The full time-series analysis results are presented in Figs. 4 and 5, as derived by both PS and SBAS using the StaMPS algorithm. The analysis shows that the metropolitan area of

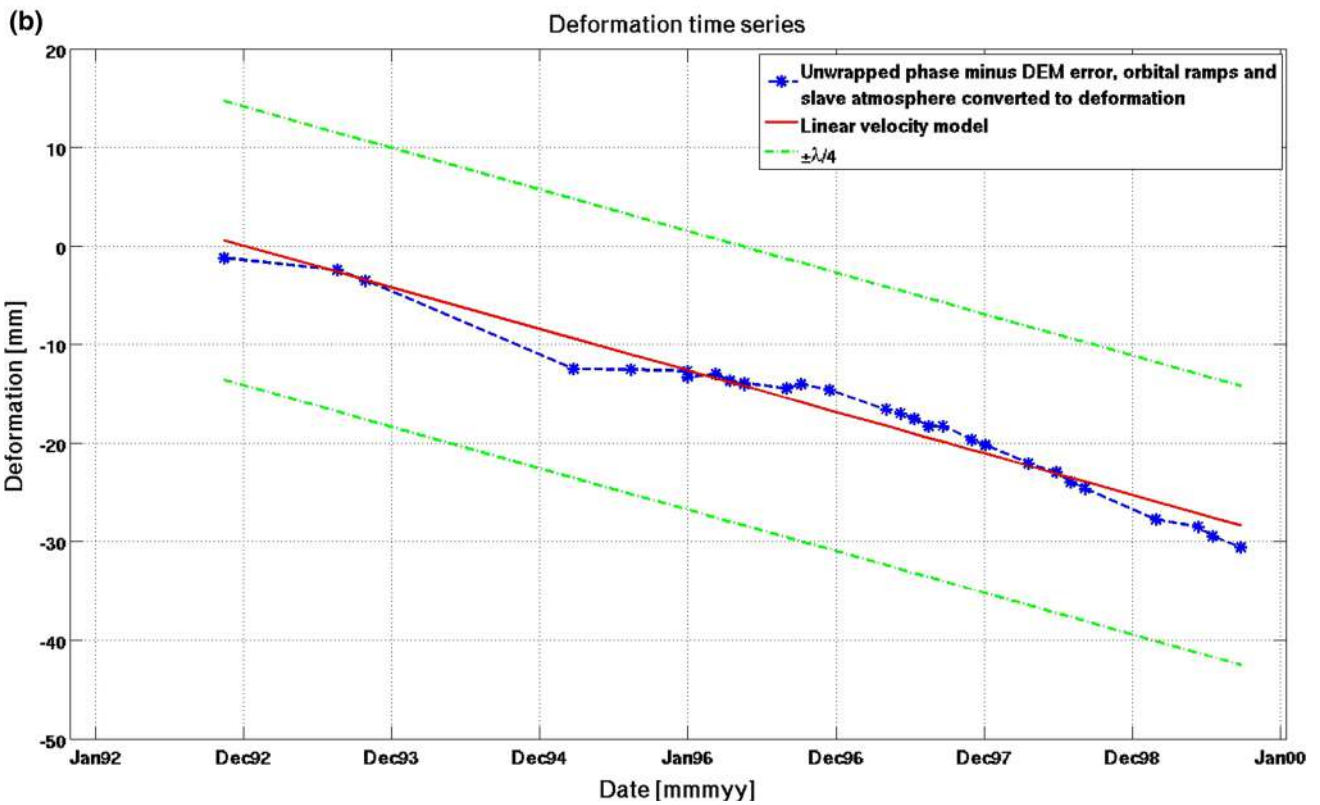
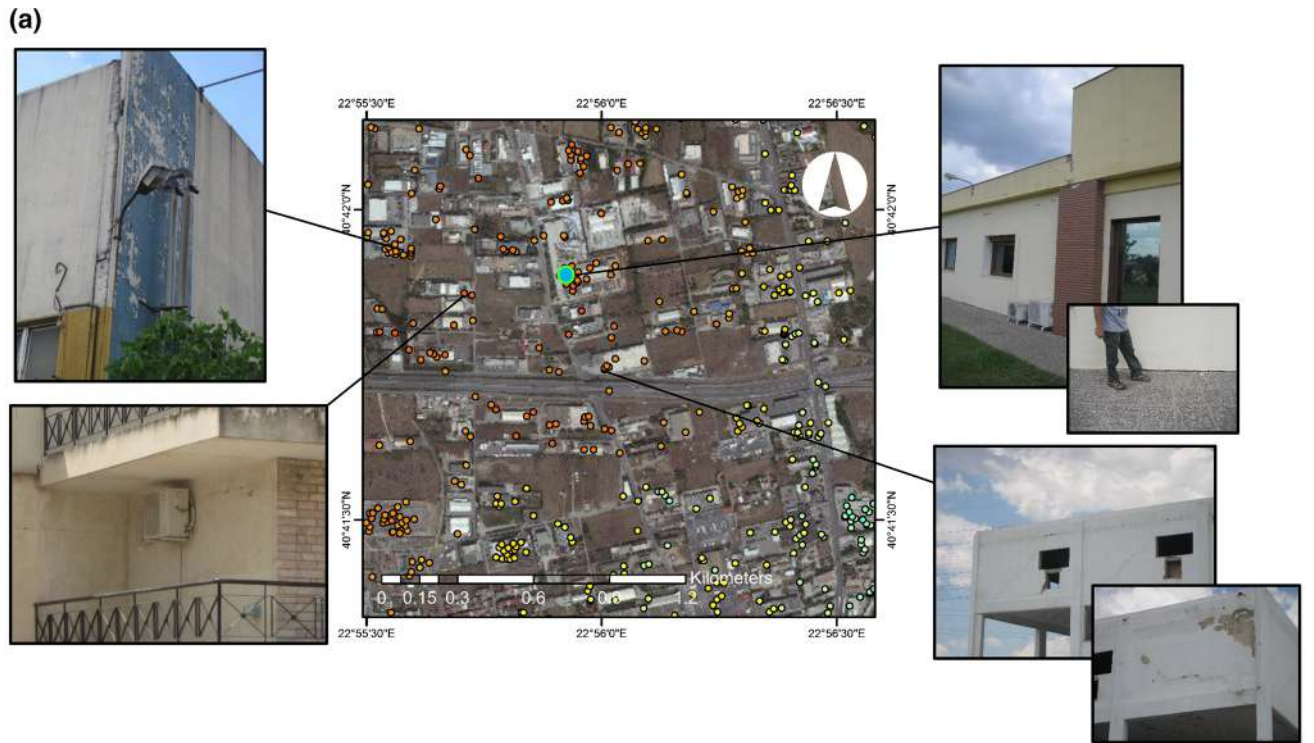
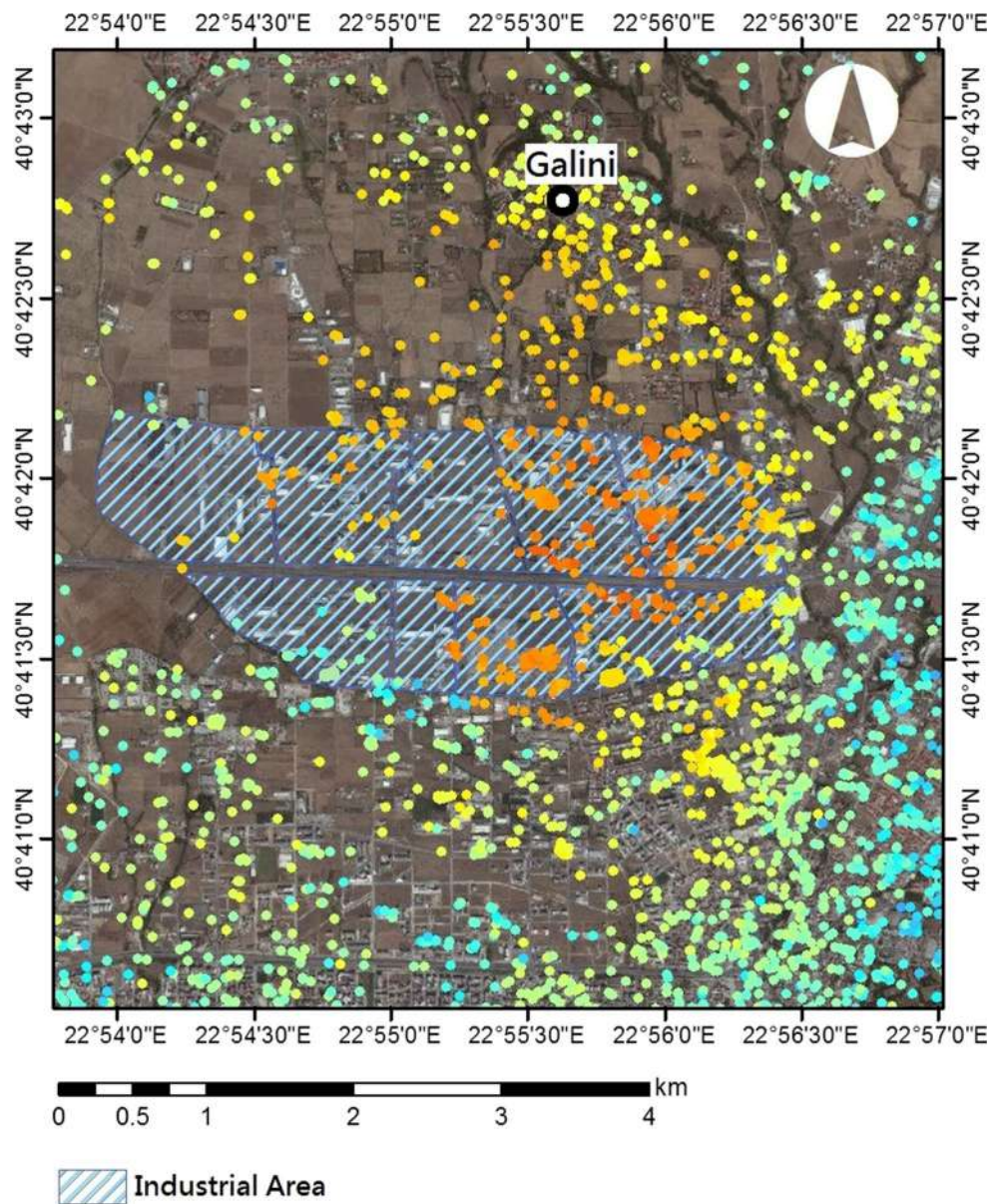


**Fig. 7** **a** Map showing the correlation of the time-series measurements of the first decade (subsidence) with failures detected in the field (*left and right*). The *light blue-light green dot* is a point whose time-series is presented in **(b)**. **b** Deformation time-series of the point in map of **(a)**

**Fig. 8** Industrial areas of Oreokastro are highlighted within the hatched polyline. The correlation of the SAR point measurements indicating the subsidence distribution (ERS dataset) with the high water demand industrial land use is in agreement with the scenario assigning the phenomena to the aquifer overpumping



Thessaloniki is relatively stable. When it comes to the area southern of Oreokastro, close to Galini, subsidence is the main deformation feature during 1992–1999, according to both PS and SBAS (Fig. 4). However, during the second decade (Fig. 5) there is a new pattern of deformation at the same area that indicates an uplift. In Fig. 6, the combined velocity result of the PS and SBAS (from StaMPS) for both decades at the broader area of Oreokastro is presented. For a further validation of the detected uplifting signal during the second decade, the same dataset was analysed using a different software; in order to cross-check the StaMPS results, the SARscape software was used for the same SAR

acquisitions. All results from all implemented techniques, from both software, are in accordance; the uplifting pattern during 2003–2010 is fully confirmed. The SARscape results can be found in the Online Resources of this study.

Repeated field inspections were performed in the area in order to chart the potential building failures that the deformation pattern might had created. Interestingly enough, the detected deforming points which were estimated from the SAR processing analysis have an absolute spatial correlation with failures detected at the industrial buildings during the field survey. In Fig. 7a, the detected building failures are presented together with the detected

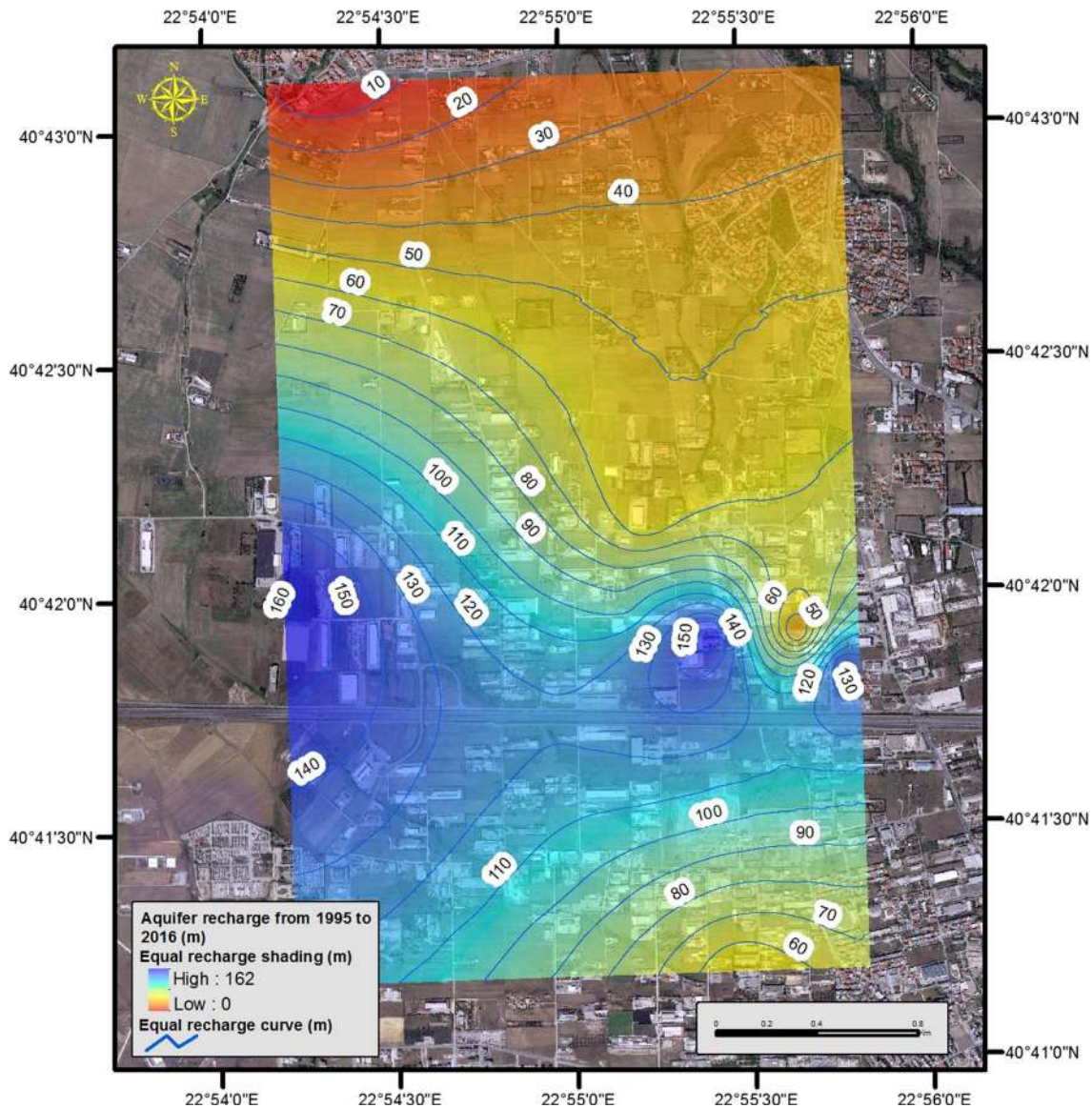


**Fig. 9** Image presenting the groundwater recharge (in m) between winter 1995 and winter 2016. Positive values of the aquifers recharge *contour* indicate recharge of the groundwater level

deforming points from 1992 to 1999 and in Fig. 7b there is a PS time-series graph of a point located at the same area. In all cases, the failures were attributed to the differential settlements of the building due to the subsidence.

## Discussion

### Driving mechanisms

For the broader industrial area of Oreokastro, one of the scenarios that previous studies have proposed as a mechanism is a connection of the deforming signal with

seismicity and fault activity. This interpretation is not supported by the magnitude of the detected deforming signal in the 90s ( $-21$  mm/year) which is far too large for this small area to be solely due to tectonic activity. The contribution of tectonic activity in the deforming signal is either zero or negligible, and for the latter case it is valid only for the period 1992–1999. The deformation history over the two decades provides interesting insights; there are extensional tectonics in the area that cannot be expressed by an uplifting surface. Thus, the scenario of tectonic activity and aseismic slip as the main driver mechanism that caused the deformation pattern at Oreokastro is rejected.



**Fig. 10** Inundation phenomena at Oreokastro due to the recovery of the underground water level (Photos taken in 2016)

Another plausible scenario for the detected deformation could be the natural compaction of the sediments. However, this phenomenon cannot take place in already consolidated or even over-consolidated Neogene formations, like the formations that occupy the narrow study area. Furthermore, this scenario is not in accordance with the change in the trend of the deforming pattern that took place during the second decade, due to the fact that, fundamentally, the subsidence due to natural compaction is irreversible. As a result, natural compaction cannot be considered as the main driving mechanism of the deformation phenomena.

Interesting conclusions can be extracted from the correlation of the land use with the deformation pattern. The focus area is one of the industrial zones of Thessaloniki. This area hosts numerous water-consuming industries such

as textile and fabric production units, mineral oil and lubricant production units, paint factories among others. For decades, the need for water was covered by municipality drills and also by private drills, in the latter case most of them illegal. This status changed in 2008 when the Thessaloniki Water Supply and Sewerage Co. SA (trading as EYATH SA) connected Oreokastro to the water supply network of Thessaloniki. Despite this fact, some private drills are still in operation, nowadays. As presented in Fig. 8, the areas with the largest amount of deformation are clearly confined within the limits of the industrial zone and as previously stated, within an area with overexploited aquifers, at least before 2008.

To further exploit these options, the hydrogeological regime of the confined aquifers of the study area was examined by evaluating measurements of the ground-

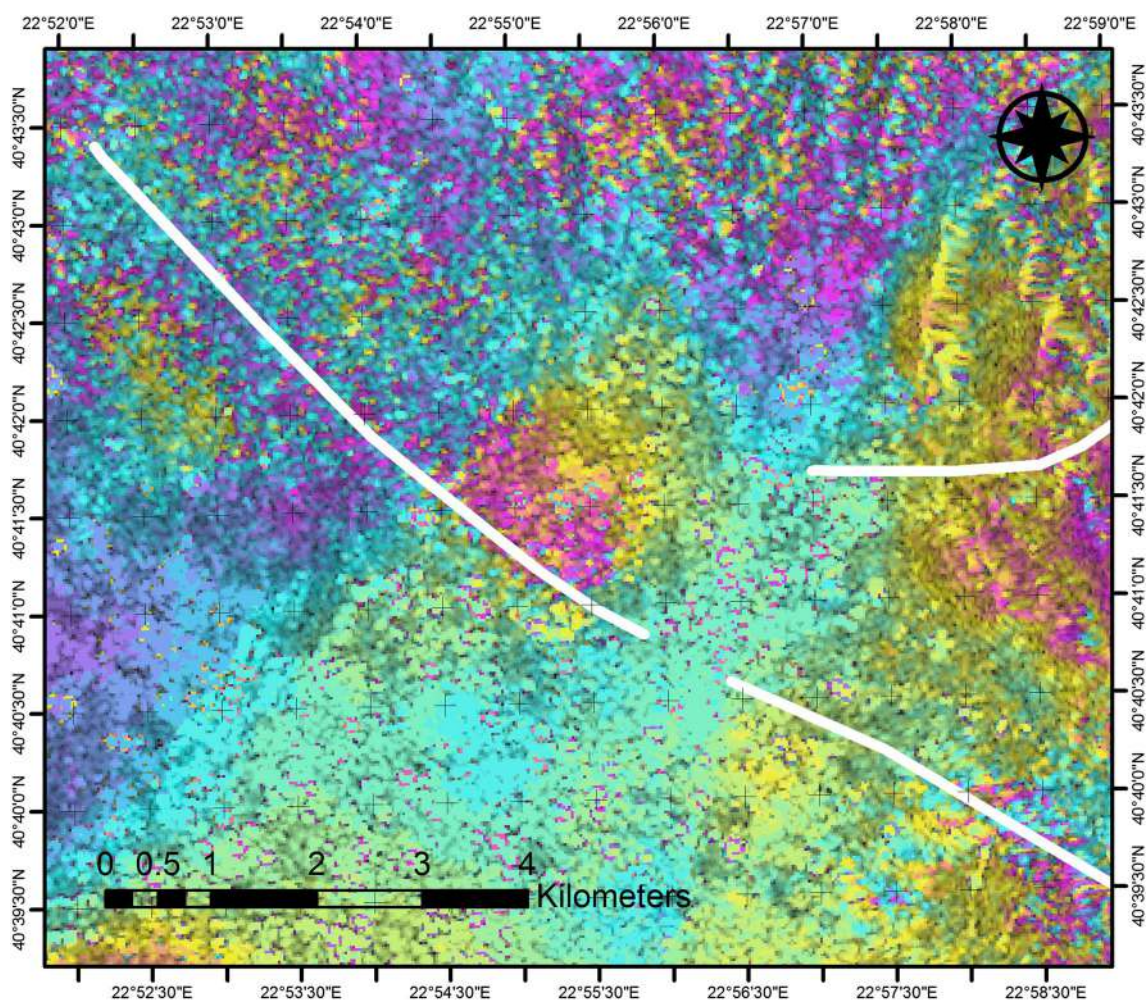


**Fig. 11** Differential interferogram presenting the interaction of the fault with the deformation pattern of Oreokastro

water level, conducted by the authors. Unfortunately, the measurements refer to random campaigns conducted since 1995 up to the present. According to these data, the aquifers, which during the 1960s were artesian, ended up at the winter of 1995 with a drawdown from  $-60$  to the maximum value of  $-200$  m. On the contrary, based on the data of the winter of 2016, the falling trend was reversed and the aquifer recovered sufficiently presenting groundwater level values from  $-10$  to  $-55$  and in some cases with artesianism. The recharge of the aquifer system is presented in Fig. 9. In order to construct the contour curves that express the spatial distribution of the groundwater recharge, Kriging techniques were utilized at the groundwater level differences (between 1995 and 2016). Kriging is a technique for making optimal, unbiased estimates of regionalized variables

at non-sampled locations using the structural properties of the semivariogram and the initial set of data values (David 1977).

The main advantage of Kriging is that it takes into consideration the spatial structure of the parameter that is investigated an approach that is not followed in other methods like arithmetic mean method, nearest neighbour method, distance weighted method and polynomial interpolation (Ly et al. 2013). Also, Kriging provides the estimation variance at every estimated point, which is an indicator of the accuracy of the estimated value (Kumar 2007).

The artesianism in the area was also expressed with inundation phenomena with limited extent (Fig. 10). This recharge could be attributed to two factors: firstly, to the establishment of a water network at the industrial area,

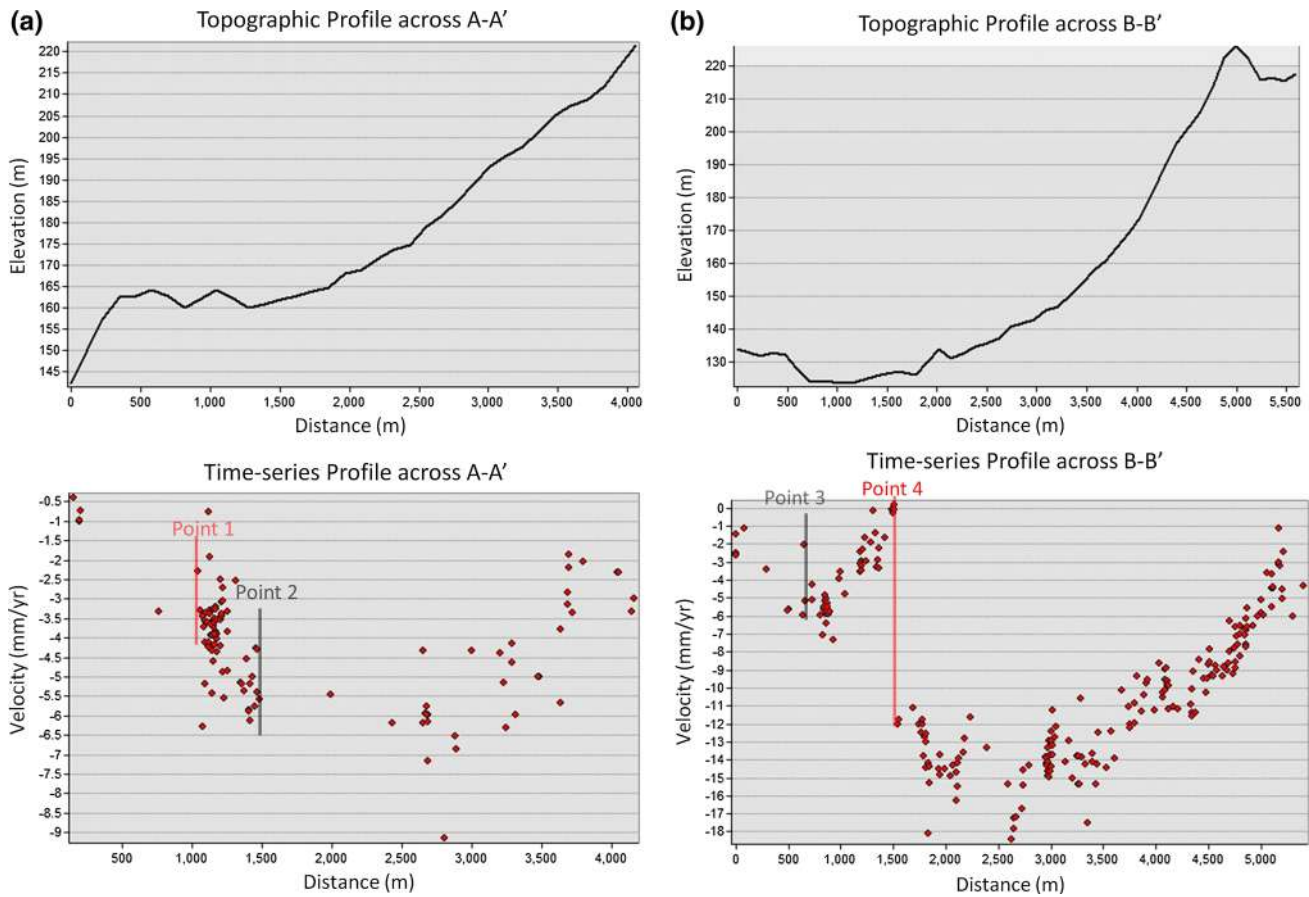


**Fig. 12** a–f Velocity and topographic profiles for the traces A–A', B–B', C–C', D–D', E–E', F–F'. The intersection of each trace's profile with the Asvestochori fault (Fig. 6) is denoted with a *black vertical*

*line*. The intersection of each trace's profile with the previously unknown structure is denoted with a *red vertical line*. Notice that in either cases there is a low or sharp disturbance in the velocities

connected with the water supply network of EYATH S.A., and secondly to the financial crisis that led numerous industries to shutdown, reducing the overall water consumption at the entire industrial zone.

Summing up, the detected deformation pattern as well as the trend eversion can be clearly combined with the hydrogeological regime of the study area and as a result the groundwater variations can be considered as the main driver mechanism of the land subsidence—uplift phenomena.

**New tectonic insights**

A thorough look at Fig. 6 shows that there is a possible relation of the faulting regime of the wider area with the deformation pattern. The deformation pattern of the

2003–2010 dataset appears to be bordered to the west by the extension of the Asvestochori fault. This can also be seen clearly from the differential interferogram presented in Fig. 11. Thus at first, the existence of the fault that was presented by structural geologists in the past is also detected via satellite-based observations. Secondly, the fact that the deformation pattern related with aquifer activity is affected by tectonic structures gives valuable information regarding the effect of the fault to the extent of the aquifers. Satellite remote sensing studies using SAR Interferometry in Las Vegas Valley, Los Angeles, Bakersfield and other areas (Amelung et al. 1999; Galloway et al. 1999; Bawden et al. 2001; Lu and Danskin 2001) indicate that the existence of faults may play an important role in the deformation pattern detected by SAR Interferometry. In our case, the pattern detected at

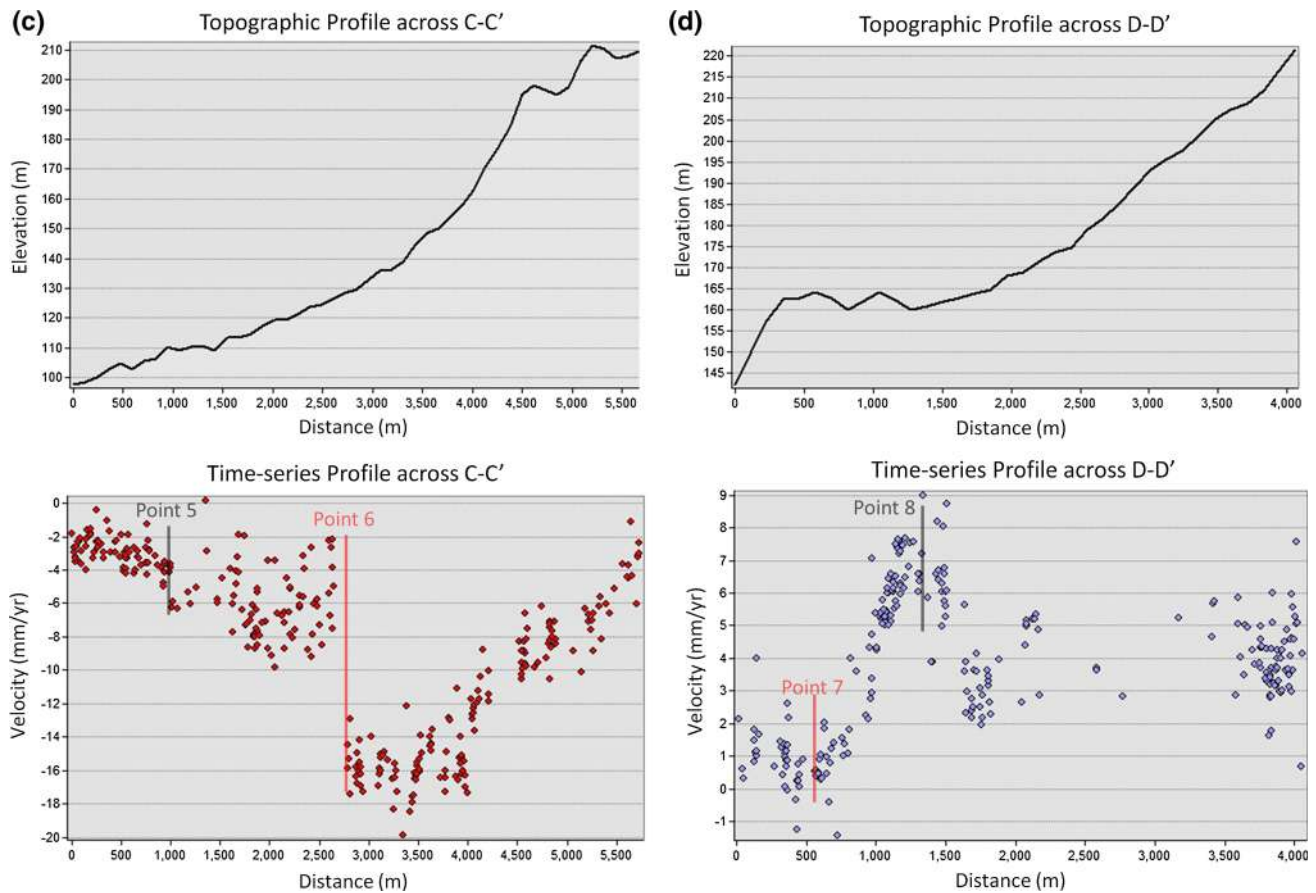


**Fig. 12** continued

the industrial area of Oreokastro appears to be a spatially fault-controlled and confined deformation (Figs. 6, 11). The extension of Asvestochori fault, south-west of Oreokastro, appears to affect radically the stratigraphy of the Neogene sediments controlling the extent and the continuity of the aquifers, practically acting as a groundwater barrier.

Moreover, the careful screening of the deformation pattern reveals a feature that is not supported by any known fault structure. More specifically, the localized uplifting deformation pattern of 2003–2010 appears to have an abrupt ending to the south-east, creating a linear feature. In order to better investigate this, but also define better the aforementioned interaction with the extension of the Asvestochori fault, a series of velocity profiles were created (Fig. 12a–f) at crucial locations together with the topographic profiles for the same traces. The profiles' surface traces (A–A', B–B', C–C', D–D', E–E', F–F') are

depicted in Fig. 6. Points 1–12 of Fig. 6 are located at areas where the profile trace cuts either the unknown linear feature or the Asvestochori fault. The points are also notated in every velocity profile. Indeed, in the velocity profiles it can be seen clearly that there is a disturbance or change of the velocity trend each time that it meets either the Asvestochori fault (these areas are notated with black vertical lines in the velocity profiles) or the proposed linear feature (these areas are notated with red vertical lines in every velocity profile). The linear feature is an unknown fault or structure that restricts the deformation pattern which is either subsiding (Fig. 12a–c) or uplifting (Fig. 12d–f). This previously unidentified structure appears to lie at the area acting, as a groundwater barrier. The proposed structure is presented in Fig. 13. A drilling or a geophysical survey campaign can be conducted at the area that would further enhance its existence.

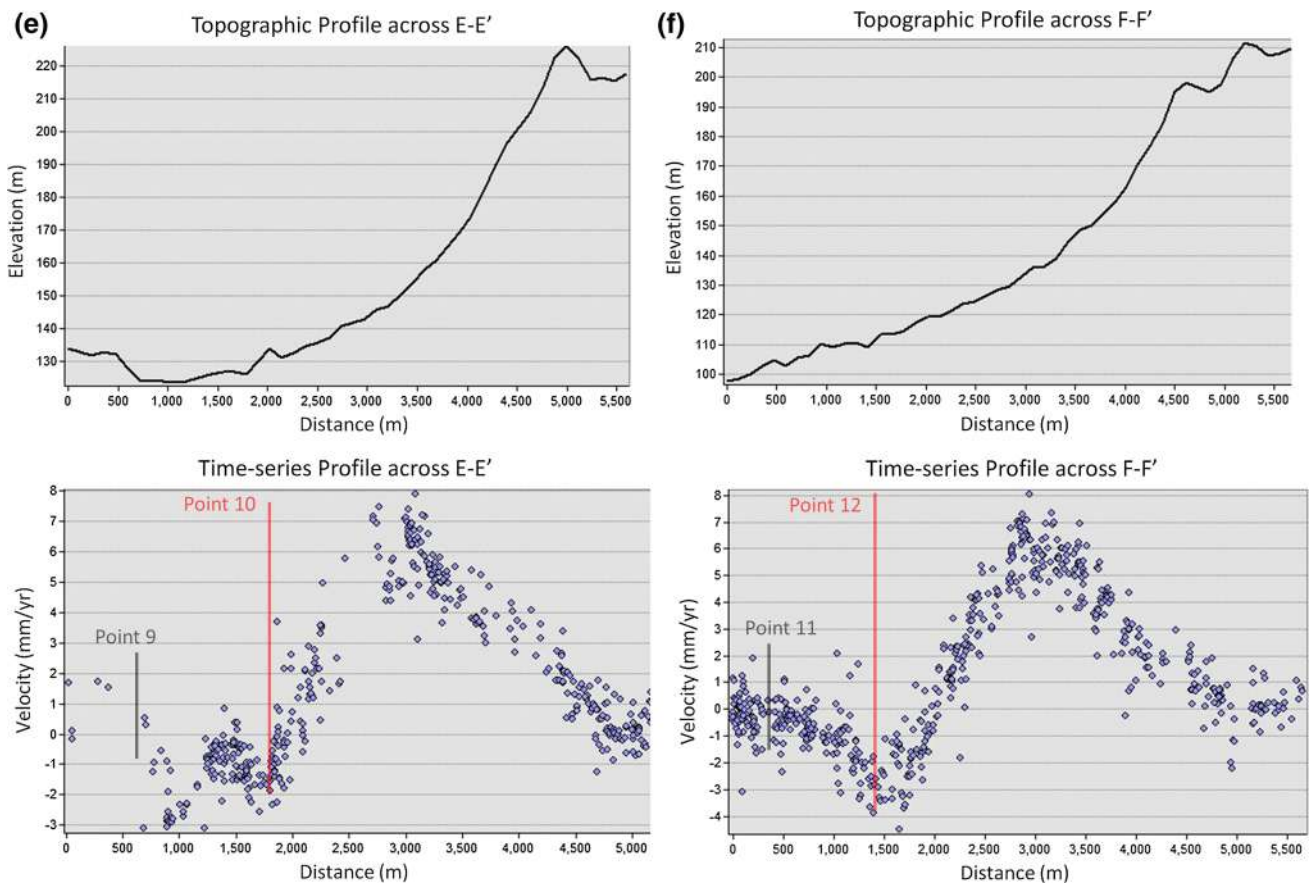


Fig. 12 continued

### Conclusions

The 1992–2010 datasets from ERS and ENVISAT are exploited to monitor the surface deformation at the wider area of Thessaloniki using a multi-technique and a multi-software approach. The focus of our study is the industrial area of Oreokastro, to the north of the city of Thessaloniki. Previous studies have captured the deformation pattern of the '90s, when studying the broader region; however, none of them focused solely to this area, to seek for a clear interpretation. During the first decade, the deformation signal indicates a clear subsidence related to the industrial activities at the broader area of Oreokastro, causing numerous failures to buildings. On the contrary, after 2000 the deforming trend has changed to uplift, a fact that made the area an intriguing case study.

Seeking for the driving mechanism, the scenario of tectonics was excluded due to the excessive deformation

rates that cannot be attributed to the tectonic activity. Furthermore, the eversion of the deformation trend from subsidence to uplift excludes the hypothesis of the natural sediment compaction, since this mechanism is irreversible.

The fact that the subsiding deformation has been confined within the limits of the industrial area with the overexploited aquifers, as well as the fact that the deformation trend changed radically to uplift when the consumption of the groundwater was reduced, sets the overexploitation of the aquifers as the main driving mechanism of the phenomena. It should be mentioned that this study is one of the few case studies worldwide where surface rebound due to the recovery of groundwater levels is thoroughly documented.

From a tectonic point of view, the shape of the deformation pattern is well correlated with the network of faults dominating the area. The satellite monitoring supports the fact that the Asvestochori fault extends towards the NW. It is

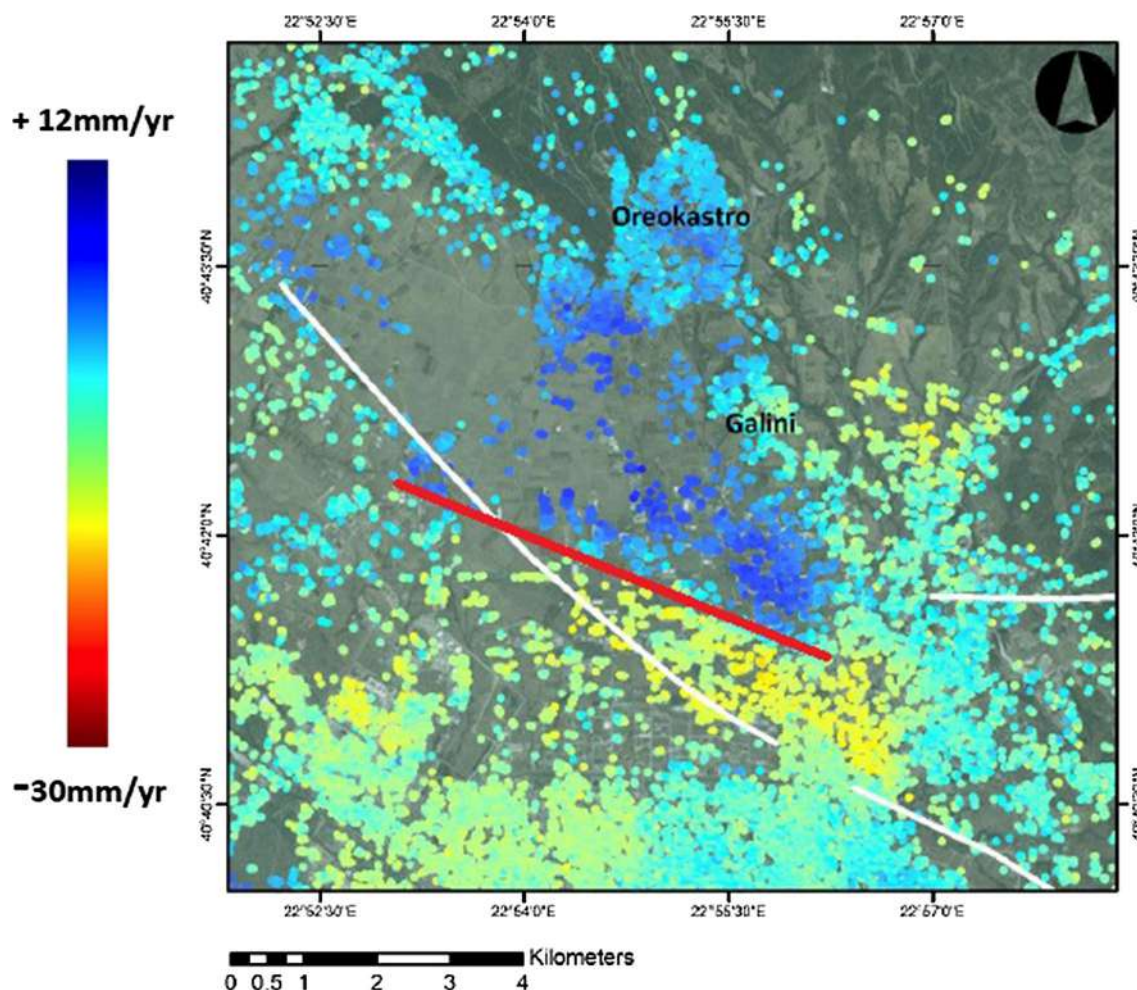


**Fig. 13** Localized deformation pattern of the second decade stops abruptly at its southern side, along a WNW–ESE linear feature, marked with the *red line*, oblique to the known fault of the region. A previously unknown structure, optimum oriented to the active stress field, appears to exist

this extension that acts as a boundary of the aquifer, rendering the detected signal as a fault-controlled deformation. Moreover, this fault-controlled deformation revealed a new, previously unknown tectonic structure. All above findings provide substantial information for the geological regime of the industrial area and its future development.

**Acknowledgements** We express our sincere gratitude to the comments and suggestions of the three reviewers and the editor, which greatly improved the initial submission. SAR data of ERS and ENVISAT are courtesy of the European Space Agency (ESA). Jeff Freymueller and Cécile Lasserre are gratefully thanked for scientific discussions. The focusing of the data was done using ROI-PAC. Doris software (by the Delft Institute of Earth Observation and Space Systems (DEOS), Delft University of Technology) was used for interferogram generation. StaMPS and SARscape for the SAR time-series processing. The study was partially funded by (a) the European Union 7th Framework Programme (FP7-REGPOT-2012-2013-1), in the framework of the project BEYOND “Building a Centre of Excellence for EO-based monitoring of Natural Disasters”, G. A. 316,210 and (b) by the European Union (European Social Fund—ESF) and Greek national funds through the Operational Program “Education and Lifelong Learning” of the National Strategic

Reference Framework (NSRF)—Research Funding Program: Thales—Investing in knowledge society through the European Social Fund (MIS377335 Prof A. Kiratzi coordinator).

## References

- Amelung F, Galloway DL, Bell JW, Zebker HA, Lacznik RJ (1999) Sensing the ups and downs of Las Vegas—InSAR reveals structural control of land subsidence and aquifer-system deformation. *Geology* 27:483–486
- Amelung F, Jónsson S, Zebker H, Segall P (2000) Widespread uplift and ‘trapdoor’ faulting on Galápagos volcanoes observed with radar interferometry. *Nature* 407:993–996
- Arnaud A, Adam N, Hanssen R, Inglada J, Duro J, Closa J, Eineder M (2003) ASAR ERS interferometric phase continuity. In: Proceedings of IGARSS 2003, France, Toulouse
- Battazza F, Ciappa A, Coletta A, Covello F, Manoni G, Pietranera L, Valentini G (2009) COSMO-SkyMed Mission: a set of X-band SAR Applications conducted during 2008. *Ital J Remote Sens* 41(3):7–21. doi:10.5721/ITJRS20094131
- Bawden GW, Thatcher W, Stein RS, Hudnut KW, Peltzer G (2001) Tectonic contraction across Los Angeles after removal of groundwater pumping effects. *Nature* 412:812–815

- Bell JW, Amelung FA, Ferretti A, Bianchi M, Novali F (2008) Permanent scatterer InSAR reveals seasonal and long-term aquifer-system response to groundwater pumping and artificial recharge. *Water Resour Res* 44(2):2407–2425
- Berardino P, Fornaro G, Lanari R, Sansosti E (2002) A new algorithm for surface deformation monitoring based on small baseline differential SAR interferograms. *IEEE Trans Geosci Remote Sens* 40(11):2375–2383
- Bianchini S, Cigna F, Righini G, Proietti C, Casagli N (2012) Landslide HotSpot mapping by means of persistent scatterer interferometry. *Environ Earth Sci* 67(4):1155–1172
- Bovenga F, Wasowski J, Nitti DO, Nutricato R, Chiaradia MT (2012) Using COSMO/SkyMed X-band and ENVISAT C-band SAR interferometry for landslides analysis. *Remote Sens Environ* 119:272–285
- Brunori CA, Bignami C, Stramondo S, Bustos E (2013) 20 years of active deformation on volcano caldera: joint analysis of InSAR and AInSAR techniques. *Int J Appl Earth Obs Geoinf* 23:279–287
- Burgmann R, Rosen PA, Fielding EJ (2000) Synthetic Aperture Radar Interferometry to Measure Earth's Surface Topography And Its Deformation. *Annu Rev Earth Planet Sci* 28:169–209
- Chen C-T, Hu J-C, Lu C-Y, Lee J-C, Chan Y-C (2007) Thirty-year land elevation change from subsidence to uplift following the termination of groundwater pumping and its geological implications in the Metropolitan Taipei Basin, Northern Taiwan. *Eng Geol* 95:30–47. doi:[10.1016/j.enggeo.2007.09.001](https://doi.org/10.1016/j.enggeo.2007.09.001)
- Cigna F, Bianchini S, Casagli N (2012a) How to assess landslide activity and intensity with persistent scatterer interferometry (PSI): the PSI-based matrix approach. *Landslides* 10:1–17
- Cigna F, Osmanoglu B, Cabral-Cano E, Dixon TH, Ávila-Olivera JA, Garduno- Monroy VH, Demets C, Wdowinski S (2012b) Monitoring land subsidence and its induced geological hazard with Synthetic Aperture Radar Interferometry: a case study in Morelia, Mexico. *Remote Sens Environ* 117:146–161
- Colesanti C, Wasowski J (2006) Investigating landslides with spaceborne Synthetic Aperture Radar (SAR) interferometry. *Eng Geol* 88(3–4):173–199
- Colesanti C, Ferretti A, Prati C, Rocca F (2003) Monitoring landslides and tectonic motion with the Permanent Scatterers technique. *Eng Geol* 68(1–2):3–14
- Costantini M, Falco S, Malvarosa F, Minati FA (2008) New method for identification and analysis of persistent scatterers in series of SAR images. In: *Proceedings of IEEE international geoscience and remote sensing symposium*, Boston, MA, USA, pp 449–452
- Costantini F, Mouratidis A, Schiavon G, Sarti F (2016) Advanced InSAR techniques for deformation studies and for simulating the PS-assisted calibration procedure of Sentinel-1 data: Case study from Thessaloniki (Greece), based on the Envisat/ASAR archive. *Int J Remote Sens*. doi:[10.1080/01431161.2015.1134846](https://doi.org/10.1080/01431161.2015.1134846)
- David M (1977) *Geostatistical ore reserve estimation*. Elsevier, Amsterdam
- Dixon TH (1994) SAR interferometry and surface change detection. Report of a workshop, Boulder, Colorado, USA
- Duro J, Closa J, Biescas E, Crosetto M, Arnaud A (2005) High resolution differential interferometry using time series of ERS and ENVISAT SAR data. In: *Proceedings of the 6th geomatic week conference*, Barcelona, Spain, 8–11 February
- EPPO (1996) Neotectonic Map of Greece, Thessaloniki sheet, scale: 1:100000
- Farina P, Colombo D, Fumagalli A, Marks F, Moretti S (2006) Permanent Scatterers for landslide investigations: outcomes from the ESA-SLAM project. *Eng Geol* 88:200–217
- Farr TG, Kobrick M (2000) Shuttle radar topography mission produces a wealth of data. *EOS Trans AGU* 81:583–585
- Ferretti A, Prati C, Rocca F (2000) Nonlinear subsidence rate estimation using permanent scatterers in differential SAR interferometry. *IEEE Trans Geosci Remote Sens* 38:2202–2212
- Ferretti A, Prati C, Rocca F (2001) Permanent scatterers in SAR interferometry. *IEEE Trans Geosci Remote Sens* 39:8–20
- Gabriel AK, Goldstein RM, Zebker HA (1989) Mapping small elevation changes over large areas: differential radar interferometry. *J Geophys Res* 94(B7):83–91
- Galloway DL, Jones DR, Ingebritsen SE (1999) Land subsidence in the United States: U.S. Geological Survey Circular 1182
- Ganas A, Oikonomou A, Tsimi C (2013) NOAFAULTS: a digital database for active faults in Greece. In: *Bulletin of the Geological Society of Greece*, vol. XLVII 2013 proceedings of the 13th International Congress, Chania
- Garlaoui C, Papadimitriou E, Karakostas V, Kilias A, Lasocki S (2015) Fault population recognition through microseismicity in Migdonia region (northern Greece). *Bollettino di Geofisica Teorica ed Applicata* 56(3):367–382
- Herrera G, Gutiérrez F, García-Davalillo JC, Notti D, Galve JP, Fernández Merodo JA, Cooksley G (2013) Multi-sensor advanced DInSAR monitoring of very slow landslides: the Tena valley case study (central Spanish Pyrenees). *Remote Sens Environ* 128:31–43
- Hooper A (2006) Persistent scatterer radar interferometry for crustal deformation studies and modeling of volcanic deformation. Ph.D. thesis, Stanford University
- Hooper A, Zebker H, Segall P, Kampes B (2004) A new method for measuring deformation on volcanoes and other natural terrains using InSAR persistent scatterers. *Geophys Res Lett* 31:1–5. doi:[10.1029/2004GL021737](https://doi.org/10.1029/2004GL021737)
- Hooper A, Segall P, Zebker H (2007) Persistent scatterer interferometric synthetic aperture radar for crustal deformation analysis, with application to Volcán Alcedo, Galápagos. *J Geophys Res* 112:B07407. doi:[10.1029/2006JB004763](https://doi.org/10.1029/2006JB004763)
- Ikehara ME, Phillips SP (1994) Determination of land subsidence related to ground-water-level declines using global positioning system and leveling surveys in Antelope Valley, Los Angeles and Kern Counties, California, 1992, U.S. Geol. Surv. Water Resour. Invest. Rep., 94-4184
- Ishitsuka K, Fukushima Y, Tsuji T, Yamada Y, Matsuoka T, Giao PH (2014) Natural surface rebound of the Bangkok plain and aquifer characterization by persistent scatterer interferometry. *Geochem Geophys Geosyst* 15:965–974. doi:[10.1002/2013GC005154](https://doi.org/10.1002/2013GC005154)
- Kampes B, Usai S (1999) Doris: the delft object-oriented radar interferometric software. In: *Proceedings of the 2nd international symposium on operationalization of remote sensing*. Enschede, The Netherlands
- Ketelaar VBH (2009) *Satellite radar interferometry: subsidence monitoring techniques*. Springer, New York (**Chapter 3**)
- Kumar V (2007) Optimal contour mapping of groundwater levels using universal kriging—a case study. *Hydrol Sci J* 52(5):1038–1050
- Lanari R, Mora O, Manunta M, Mallorquì JJ, Berardino P, Sansosti E (2004) A small baseline approach for investigating deformation on full resolution differential SAR interferograms. *IEEE Trans Geosci Remote Sens* 42(7):1377–1386
- Liu P, Li ZH, Hoey T, Kincal C, Zhang JF, Zeng QM, Muller J (2013) Using advanced InSAR time series technique to monitor landslide movements in Badong of the three Gorges region, China. *Int J Appl Earth Obs Geoinf* 21:253–264
- Lu Z, Danskin WR (2001) InSAR analysis of natural recharge to define structure of a ground-water basin, San Bernardino, California. *Geophys Res Lett* 28:2661–2664
- Ly S, Charles C, Degré A (2013) Different methods for spatial interpolation of rainfall data for operational hydrology and

- hydrological modeling at watershed scale. A review. *Biotechnol Agron Soc Environ* 17(2):392–406
- Massonnet D (1997) Satellite radar interferometry. *Sci Am* 276(2):46–53
- Massonnet D, Feigl K (1998) Radar interferometry and its application to changes in the Earth's surface. *Rev Geophys* 36:441–500
- Massonnet D, Rossi M, Carmona C, Adragna F, Peltzer G, Feigl K, Rabaute T (1993) The displacement field of the Landers earthquake mapped by radar interferometry. *Nature* 364:138–142
- Mora O, Mallorquí JJ, Broquetas A (2003) Linear and nonlinear terrain deformation maps from a reduced set of interferometric SAR images. *IEEE Trans Geosci Remote Sens* 41:2243–2253
- Mouratidis A (2010) Contribution of GPS and GIS-assisted spaceborne remote sensing in the morphotectonic research of Central Macedonia (N. Greece), Ph.D. thesis, Aristotle University of Thessaloniki
- Mouratidis A, Costantini F, Votsis A (2011) Correlation of DInSAR deformation results and active tectonics in the city of Thessaloniki (Greece). In: Stilla U, Gamba P, Juergens C, Maktav D (eds) JURSE 2011—Joint urban remote sensing event—Munich, Germany, April 11–13, 2011, IEEE, pp 421–424
- Papazachos C, Soupios P, Savvaidis A, Roumelioti Z (2000) Identification of small-scale active faults near metropolitan areas: an example from the Asvestochori fault near Thessaloniki. In: Proceedings of XXXII ESC General Assembly, Lisbon, Portugal, pp 221–225
- Paradisopoulou PM, Karakostas VG, Papadimitriou EE, Tranos MD, Papazachos CB, Karakaisis GF (2006) Microearthquake study of the broader Thessaloniki area (Northern Greece). *Ann Geophys* 49(4/5):1081–1093
- Parsons B, Wright T, Rowe P, Andrews J, Jackson J, Walker R, Khatib M, Talebian M, Bergman E, Engdahl ER (2006) The 1994 Sefidabeh (eastern Iran) earthquakes revisited: new evidence from satellite radar interferometry and carbonate dating about the growth of an active fold above a blind thrust fault. *Geophys J Int*. doi:10.1111/j.1365-246X.2005.02655
- Raspini F, Loupasakis C, Rozos D, Moretti S (2013) Advanced interpretation of land subsidence by validating multi-interferometric SAR data: the case study of the Anthemountas basin (northern Greece). *Nat Hazards Earth Syst Sci* 13(10):2425–2440
- Raspini C, Loupasakis C, Rozos D, Adam N, Moretti S (2014) Ground subsidence phenomena in the Delta municipality region (Northern Greece): Geotechnical modeling and validation with Persistent Scatterer Interferometry. *Int J Appl Earth Obs Geoinf* 28:78–89
- Raucoules D, Parcharidis I, Feurer D, Novalli F, Ferretti A, Carnec C, Lagios E, Sakkas V, Le Mouelic S, Cooksley G (2008) Ground deformation monitoring of the broader area of Thessaloniki (Northern Greece) using radar interferometry techniques. *Nat Hazards Earth Syst Sci* 8:779–788
- Sonobe R, Tani H, Wang X, Kobayashi N, Kimura A, Shimamura H (2014) Application of Multi-temporal TerraSAR-X Data to Map Winter Wheat Planted Areas in Hokkaido, Japan. *JARQ* 48(4):465–470
- Sousa JJ, Hooper AJ, Hanssen RF, Bastos LC, Ruiz AM (2011) Persistent scatterer InSAR: a comparison of methodologies based on a model of temporal deformation vs. spatial correlation selection criteria. *Remote Sens Environ* 115(10):2652–2663
- Svigkas N, Papoutsis I, Loupasakis K, Kontoes H, Kiratzi A (2015) Geo-hazard monitoring in northern Greece using InSAR techniques: the case Study of Thessaloniki, (Abstract ID33). In: 9th International Workshop Fringe 2015 “Advances in the Science and Applications of SAR Interferometry and Sentinel-1 InSAR”, ESA-ESRIN, Frascati, Italy, 23–27 March 2015
- Svigkas N, Papoutsis I, Loupasakis C, Tsangaratos P, Kiratzi A, Kontoes CH (2016) Land subsidence rebound detected via multi-temporal InSAR and ground truth data in Kalochori and Sindos regions, Northern Greece. *Eng Geol*. doi:10.1016/j.enggeo.2016.05.017
- Taniguchi M, Shimada J, Fukuda Y, Yamano M, Onodera S, Kaneko S, Yoshikoshi A (2009) Anthropogenic effects on the subsurface thermal and ground water environments in Osaka, Japan and Bangkok, Thailand. *Sci Total Environ* 407(9):3153–3164. doi:10.1016/j.scitotenv.2008.06.064
- van der Kooij M, Hughes W, Sato S, Poncos V (2006) Coherent target monitoring at high spatial density: examples of validation results. In: European Space Agency Special Publications, SP-610
- Wright P, Stow R (1999) Detecting mining subsidence from space. *Int J Remote Sens* 20(6):1183–1188
- Wright TJ, Parsons B, Jackson J, Haynes M, Fielding E, England P, Clarke P (1999) Source parameters of the 1 October 1995 Dinar (Turkey) earthquake from SAR interferometry and seismic bodywave modelling. *Earth Planet Sci Lett* 172:23–37
- Wright TJ, Fielding EJ, Parsons BE, England PC (2001) Triggered slip: observations of the 17 August 1999 Izmit (Turkey) earthquake using radar interferometry. *Geophys Res Lett* 28:1079–1082
- Wright TJ, Lu Z, Wicks C (2003) Source model for the M w 6.7, 23 October 2002, Nenana Mountain Earthquake (Alaska) from InSAR. *Geophys Res Lett* 30(18):1974. doi:10.1029/2003GL018014
- Zebker HA, Goldstein RM (1986) Topographic Mapping from Interferometric Synthetic Aperture Radar Observations. *J Geophys Res* 91(B5):4993–4999
- Zervopoulou A (2010) Neotectonic faults in the broader area of Thessaloniki, in relation to the foundation soils, Ph.D. thesis, Aristotle University of Thessaloniki (in Greek)
- Zervopoulou A, Pavlides S (2005) Morphotectonic study of the broader area of Thessaloniki for the cartography of neotectonic faults. *Bull Greek Geol Soc* 38:30–41 (in Greek)

## *Environmental Earth Sciences*

Online Supplementary material for:

### **InSAR time-series monitoring of ground displacement trends in an industrial area (Oreokastro - Thessaloniki, Greece): detection of natural surface rebound and new tectonic insights**

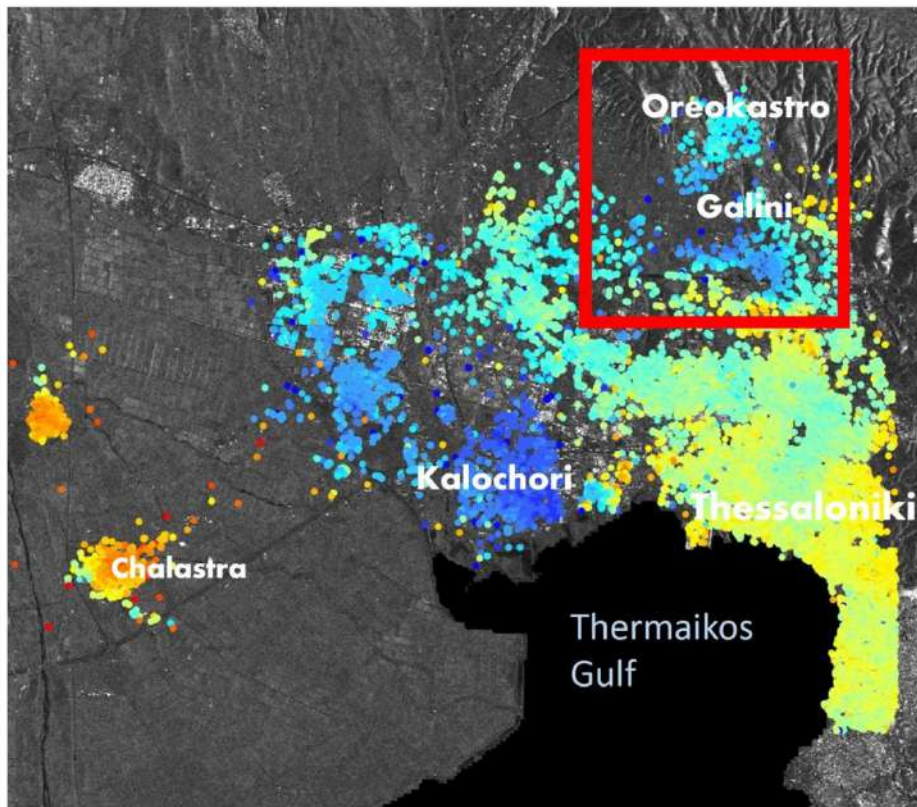
***Nikos Svigkas<sup>1,2</sup>, Ioannis Papoutsis<sup>2</sup>, Constantinos Loupasakis<sup>3</sup>, Paraskevas Tsangaratos<sup>3</sup>, Anastasia Kiratzi<sup>1</sup>, Charalampos (Haris) Kontoes<sup>2</sup>***

- (1) Department of Geophysics, Aristotle University of Thessaloniki, 54124, Thessaloniki, Greece
- (2) Institute of Space Applications and Remote Sensing, National Observatory of Athens, Athens, Metaxa & Vas. Pavlou, 15236, Athens, Greece
- (3) Laboratory of Engineering Geology and Hydrogeology, Department of Geological Sciences, School of Mining and Metallurgical Engineering, National Technical University of Athens, Zographou Campus, Heroon Polytechniou 9, 157 80, Athens, Greece

Corresponding author: Nikos Svigkas (svigkas@geo.auth.gr)

### **Introduction**

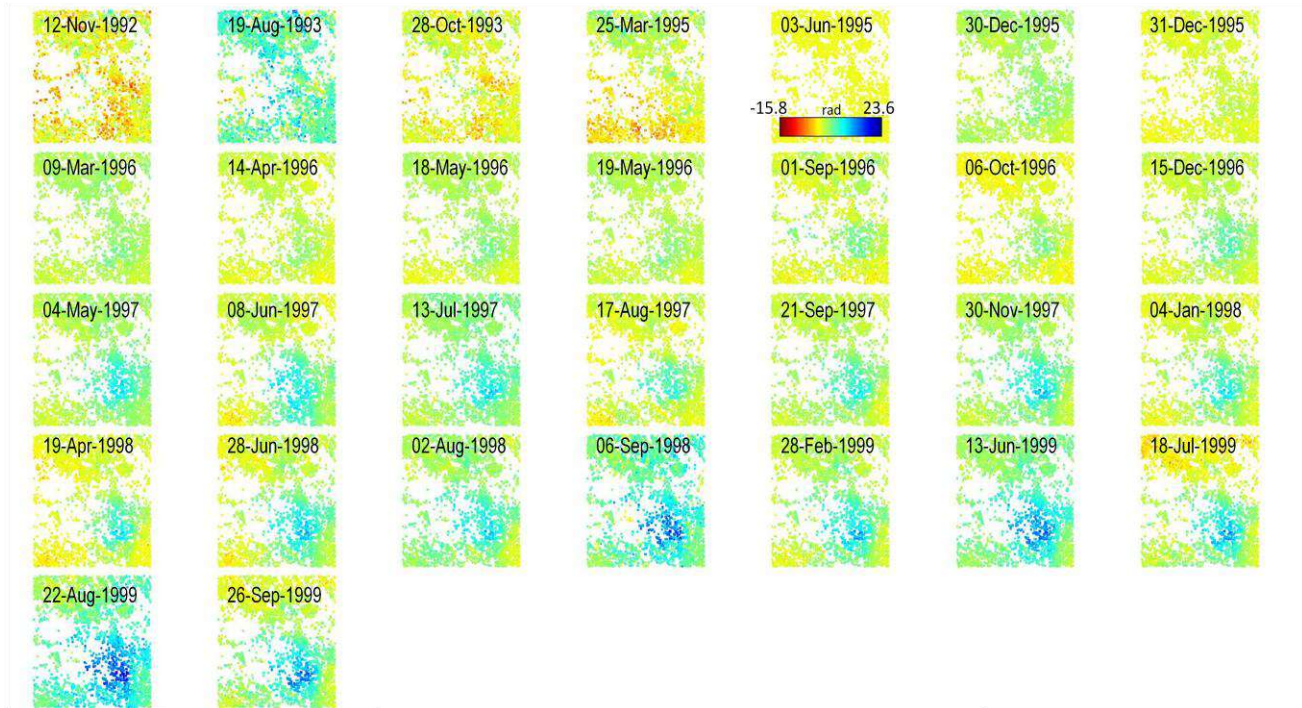
In this electronic supplementary material, in ESM\_1, additional SAR time-series results for the time span 2003-2010 are presented. These are results that derived from the analysis of the SARscape software in order to further validate the uplifting trend detected in the StaMPS results of the same dataset. Also, unwrapped interferograms of the StaMPS analysis of the ERS 1,2 and ENVISAT satellites are shown in ESM\_2 (the spatial area covering is on map in ESM\_3). In ESM\_4 and ESM\_5 the ERS and ENVISAT SLC connection graphs are shown. Tables with datasets are in ESM\_6 and ESM\_7. Finally another example that proves the deformation-fault interaction in Oreokastro, is shown in ESM\_8.



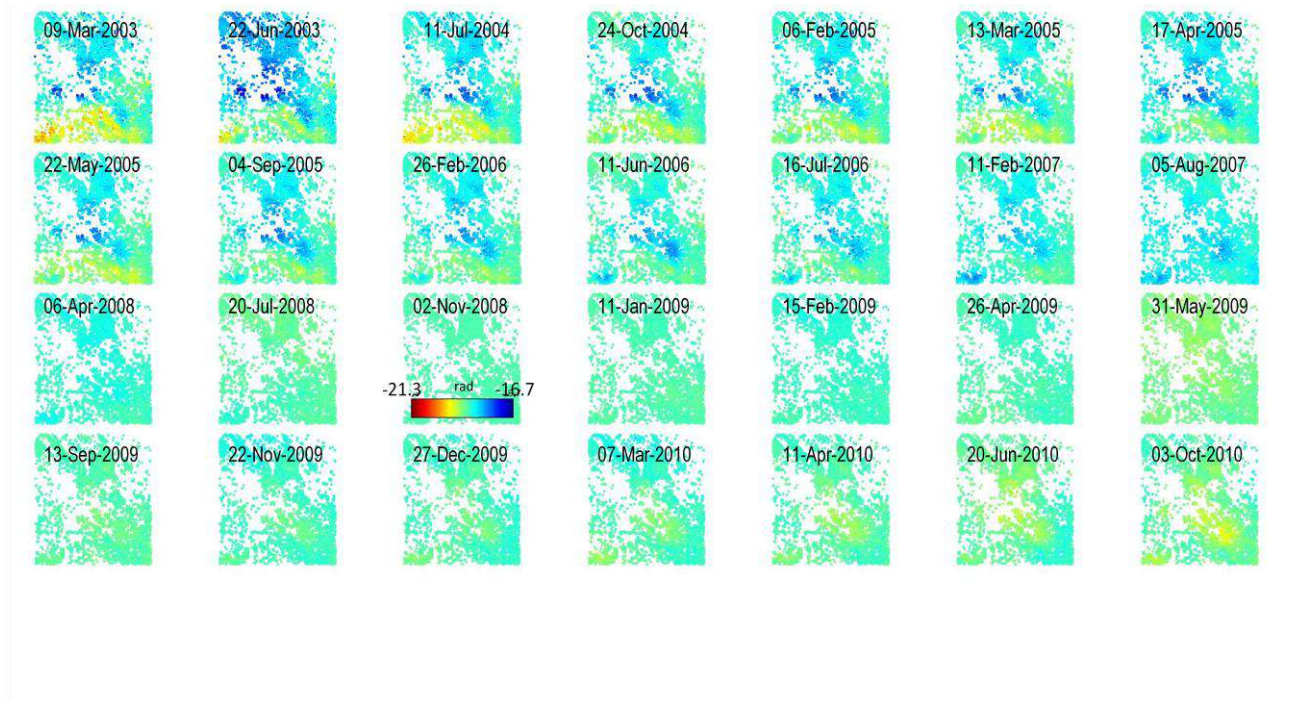
-21 mm/yr  +11 mm/yr

**ESM\_1** Results of PS processing at the broader area of study held with the SARscape software. The time span of the ENVISAT dataset is from 2003 to 2010. With the red rectangle, the area of interest of this study is denoted. As it can be seen, the industrial area of Oreokastro is under uplift. The SARscape results come in full accordance with those of StaMPS that are presented in the main text; the detected uplifting pattern is fully validated

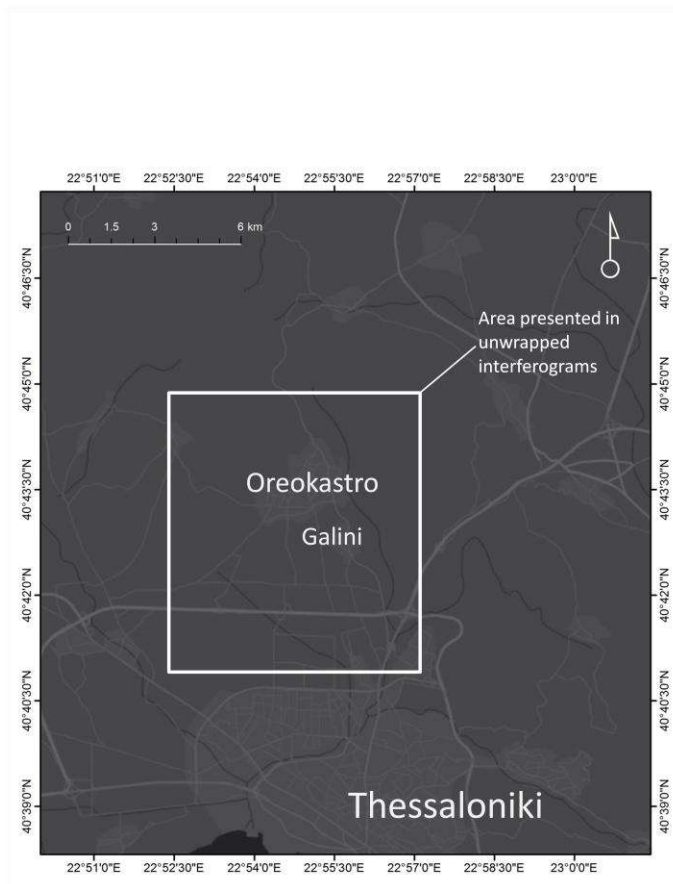
### ERS unwrapped



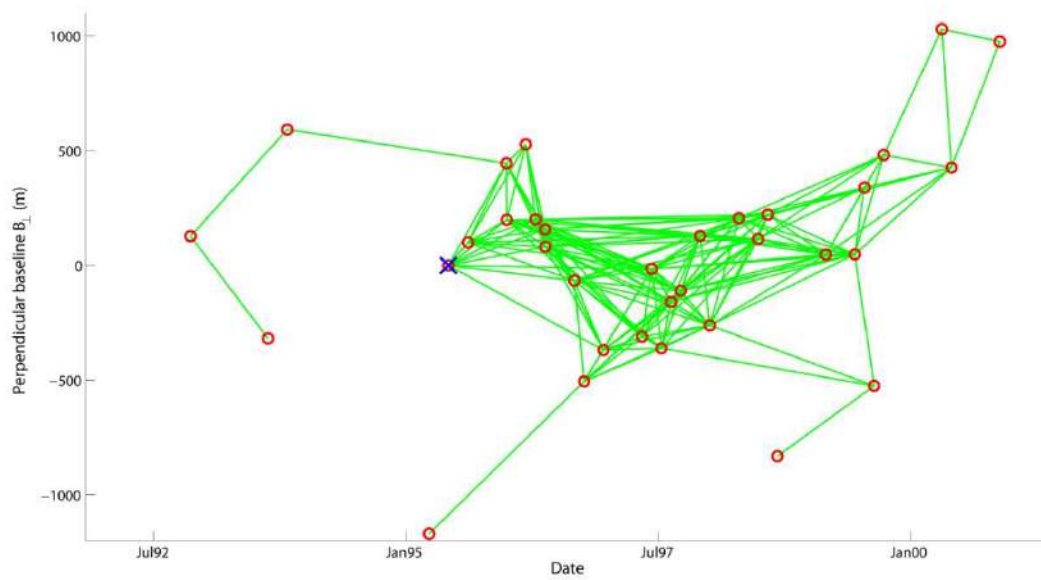
### ENVISAT unwrapped



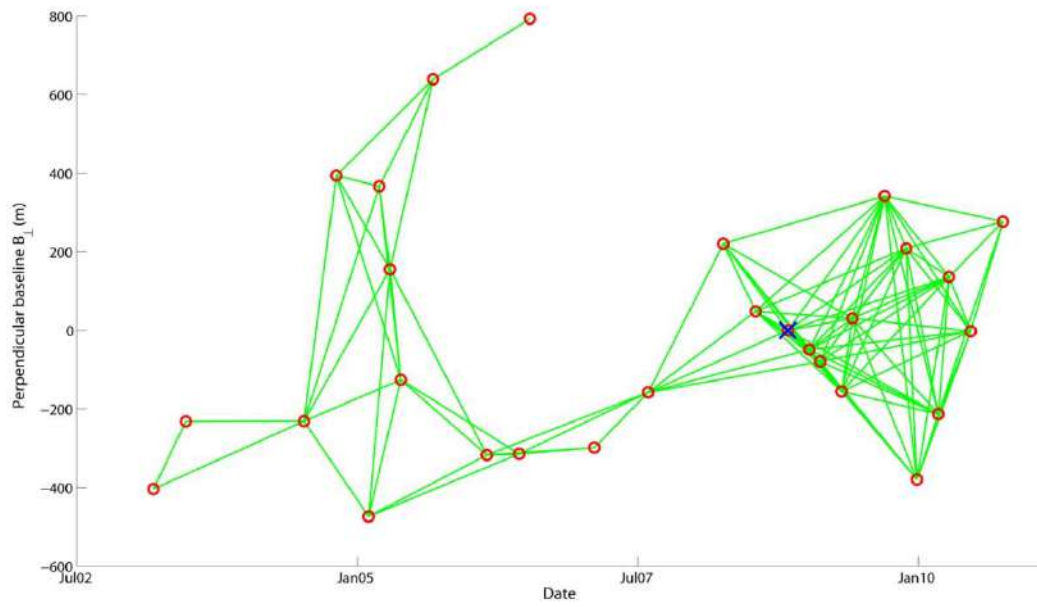
ESM\_2 StaMPS Unwrapped Interferograms of ERS 1,2 & ENVISAT



**ESM\_3** Area of unwrapped interferograms presented in ESM\_2



**ESM\_4** StaMPS SLC connection graph for ERS 1,2 satellites



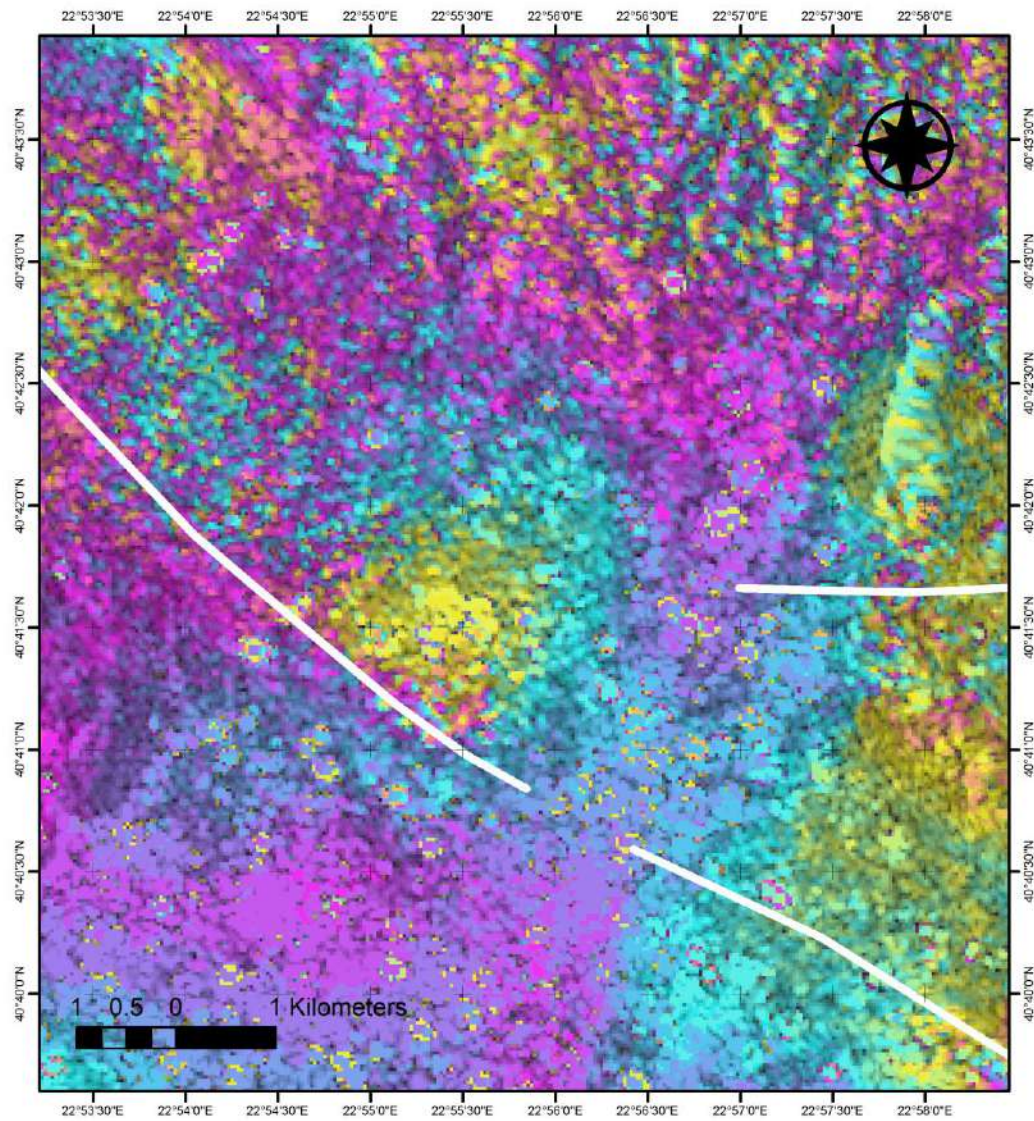
ESM\_5 StaMPS SLC connection graph for ENVISAT satellite

**ESM\_6** ERS dataset that was used in the time-series analysis

Dates	Perp. Baseline(m)	$\Delta t$ (days)
12-Nov-92	127 m	-933
19-Aug-93	-318 m	-653
28-Oct-93	593 m	-583
03-Jun-95	0 m	0
13-Aug-95	100 m	71
30-Dec-95	445 m	210
31-Dec-95	199 m	211
09-Mar-96	527 m	280
14-Apr-96	201 m	316
18-May-96	157 m	350
19-May-96	82 m	351
01-Sep-96	-67 m	456
06-Oct-96	-506 m	491
15-Dec-96	-369 m	561
04-May-97	-310 m	701
08-Jun-97	-15 m	736
13-Jul-97	-361 m	771
17-Aug-97	-158 m	806
21-Sep-97	-110 m	841
30-Nov-97	129 m	911
04-Jan-98	-261 m	946
19-Apr-98	206 m	1051
28-Jun-98	116 m	1121
02-Aug-98	221 m	1156
06-Sep-98	-831 m	1191
28-Feb-99	47 m	1366
13-Jun-99	48 m	1471
18-Jul-99	340 m	1506
22-Aug-99	-525 m	1541
26-Sep-99	481 m	1576

**ESM\_7** ENVISAT dataset that was used for the time-series analysis

Dates	Perp. Baseline(m)	$\Delta t$ (days)
9-Mar-03	-404	-2065
22-Jun-03	-232	-1960
11-Jul-04	-231	-1575
24-Oct-04	394	-1470
6-Feb-05	-474	-1365
13-Mar-05	366	-1330
17-Apr-05	156	-1295
22-May-05	-126	-1260
4-Sep-05	639	-1155
26-Feb-06	-317	-980
11-Jun-06	-314	-875
16-Jul-06	793	-840
11-Feb-07	-298	-630
5-Aug-07	-158	-455
6-Apr-08	221	-210
20-Jul-08	48	-105
2-Nov-08	0	0
11-Jan-09	-49	70
15-Feb-09	-79	105
26-Apr-09	-155	175
31-May-09	31	210
13-Sep-09	342	315
22-Nov-09	209	385
27-Dec-09	-379	420
7-Mar-10	-213	490
11-Apr-10	136	525
20-Jun-10	-2	595



**ESM\_8** Another DInSAR example of deformation-fault interaction in the area of Oreokastro